THE UNIVERSITY OF ALBERTA

EXCITATION AND RELAXATION OF THE UPPER LASER STATE

IN A CO_2 DISCHARGE

A Thesis

Submitted to the Faculty of Graduate Studies

in Partial Fulfilment of the Requirements

for the Degree of Master of Science

DEPARTMENT OF ELECTRICAL ENGINEERING

by

BERNARD MARIE EDMOND CHRISTOPHE

EDMONTON, ALBERTA.

FALL, 1970.

UNIVERSITY OF ALBERTA

FACULTY OF GRADUATE STUDIES

The undersigned certify that they have read and recommend to the Faculty of Graduate Studies for acceptance a thesis entitled "EXCITATION AND RELAXATION OF THE UPPER LASER STATE IN A CO_2 DISCHARGE," submitted by BERNARD MARIE EDMOND CHRISTOPHE in partial fulfilment of the requirements for the degree of Master of Science.

Date 12th Aug. 70

ERRATA

Page 18	line 18	read 380 ± 40 sec^{-1} $torr^{-1}$
Page 55	eq. 10, 11	ρ missing in exp:
Page 65	line 9	read much and not mush
	line 15	read band and not bound
Page 71	Remove E from $\not{E}\sqrt{E}$	

ABSTRACT

An experiment designed to measure excitation and relaxation of the upper laser level of a CO_2 under discharge conditions is described.

CO_2 molecular and $\dot{CO}_2$ deactivation processes are presented and the experimental set-up is tested by measuring known relaxation times in CO_2 and of CO_2-N_2 mixtures. A new value for CO_2-CO collision rate is also measured.

The discharge effect on the level of 4.3μ fluorescence and deactivation rate of the (001) level was investigated and found to be significant. In particular, the electron rate is comparable to molecular collisions in relaxation. Finally a theoretical quantum mechanical calculation was performed on electron excitation and de-excitation cross-sections of the upper laser level of CO_2.

ACKNOWLEDGMENTS

The author wishes to express his thanks to A.A. Offenberger who supervised his work and helped with the composition of this thesis.

Special thanks must go to T.K. Bauer who realized different instruments needed in this experiment and to B.W. Arnold who provided all the necessary optics.

The author is indebted to the Department of Electrical Engineering and to the University of Alberta for financial support.

Tout particulierement l'auteur remercie les personnes qui ont permis sa venue ici et tous les amis qui ont rendu son sejour et celui de sa femme, au Canada, si agreable.

Finally, the author would like to express his appreciation to his wife, Dominique whose patience and help have been a constant source of encouragement.

TABLE OF CONTENTS

LIST OF FIGURES

INTRODUCTION

The operation of a low pressure electrically excited CO_2 laser depends on the transfer of energy by electron and molecular collisions. The inversion of population between the upper and lower lasing levels of the CO_2 molecule (in a CO_2-N_2 mixture) is built up by the transfer of energy from vibrationally excited nitrogen molecules (by electron collision) to the antisymmetric vibrational mode of the CO_2 molecules. The addition of some gases such as helium helps the deactivation of the lower level. To compute the efficiency of the laser, knowledge of the N_2-CO_2 energy transfer cross-section must be known as well as deactivation rates for the upper and lower laser levels. (see ref. XI for complete bibliography on CO_2 laser).

Though relaxation via molecular collisions has been extensively considered, both theoretically and experimentally, relatively little attention has been paid to the influence of the plasma discharge on excitation and relaxation. This thesis is particularly concerned with such effects. In this experiment we use the CO_2 laser as a device to study the CO_2 molecule and particularly the rate of deactivation of the upper level under different conditions involved in the CO_2 laser. This study was done in three stages: the first involved the measurement of the relaxation rate of CO_2 molecules by CO_2 molecules; the second stage was concerned with determining the effect of different gases such as nitrogen and carbon monoxide on this deactivation rate; finally the effect of a glow discharge, typical of CO_2 lasers, on the relaxation was investigated.

Outlines of the Experiment

This experiment is based on the resonant absorption by CO_2 molecules, of Q-switched 10.6μ radiation and measurement of the resulting fluorescence. This method of laser excited vibrational fluorescence has already been applied to pure CO_2 by Hocker et al, Moore et al and by Rosser et al (see Ref. II, IV, V, and III).

A small cell of 2cm diameter containing CO_2 only or with other gases and able to support a discharge is placed inside or outside an actively Q-switched CO_2-N_2-H_e laser cavity (see Fig. I). The cell is closed at both ends by two salt windows at the Brewster angle. A salt window on the side is used to monitor the infra-red fluorescence. The cell is small enough that even when placed inside the laser cavity it is not going to perturb the gain of the much longer CO_2 laser.

The cavity of the laser is set between a 10 m radius gold coated mirror when the cell is placed inside or a germanium mirror when the cell is outside, and a rotating flat gold mirror. This rotation is generated by an air turbine with an adjustable speed from 0 to 24000 rpm, resulting in Q-spoiled pulses of the order of 1 μsec width. It is possible using the AC (800 Hz) excited laser itself to determine the fluorescence time constant. This is accomplished by measuring the phase difference between the 10.6μ pump radiation and the 4.3μ fluorescence using a lock-in amplifier locked to 800 Hz. The Q-switched technique, however allows more reliable measurements and was therefore used for these studies.

Two detectors have been used, a mercury doped germanium and

EXPERIMENTAL SET-UP

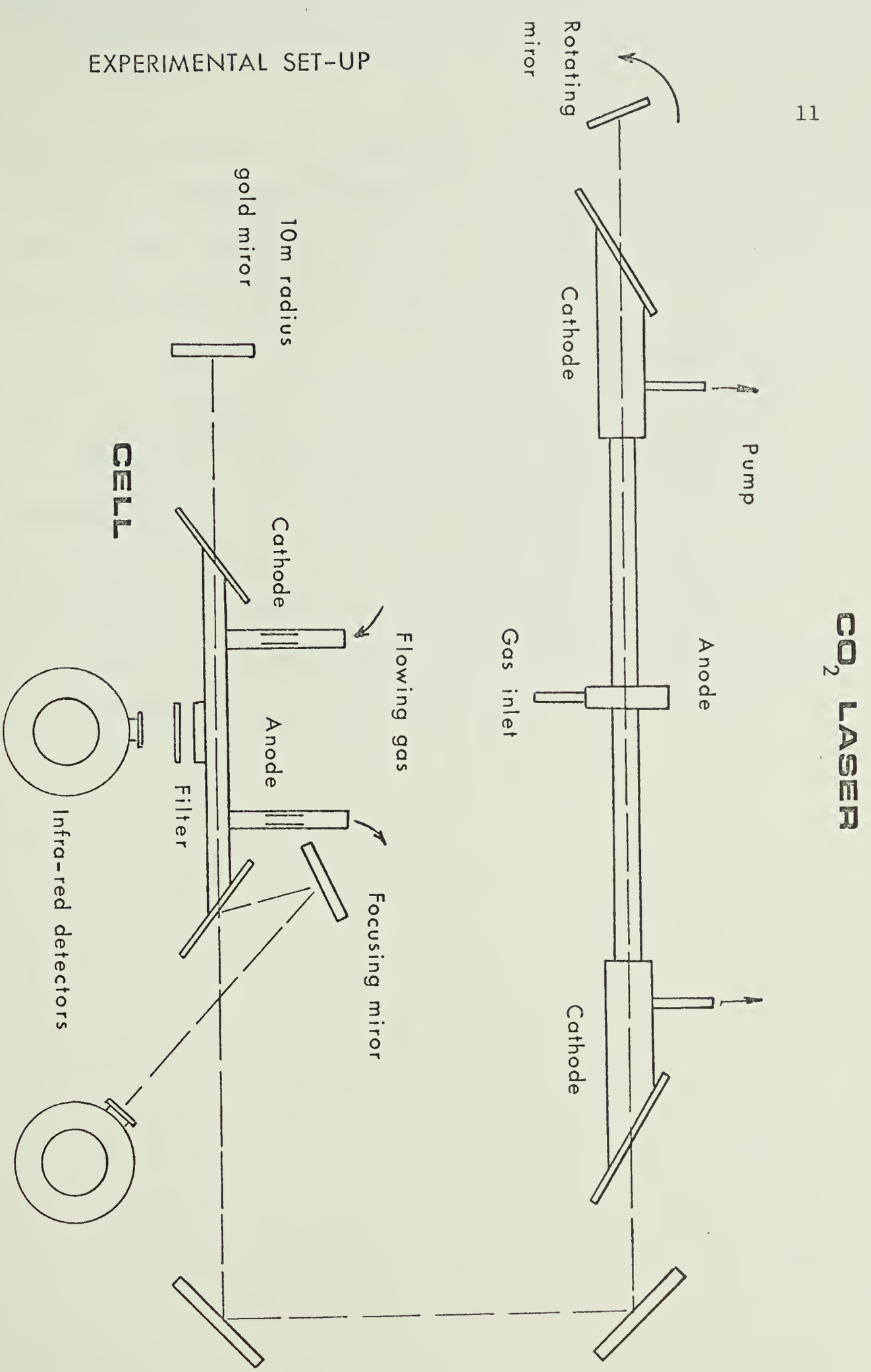

FIG. 1

a gold doped germanium, the latter with a calcium fluoride window to reduce the scattered radiation at 10.6μ. Both detectors give almost the same sensitivity at 4.3μ. They both have shown the same circuitry rise time of the order of 1 μsec.

Also, various filters and a monochromator were used to monitor the wavelengths of the infra-red emission. The signal was either directly displayed on a 556 dual beam oscilloscope or determined using a lock-in amplifier locked to 800 Hz. Important variables such as pressure and temperature were monitored using a Wallace-Tiernan gauge and an iron-constantan thermocouple. Probe measurements of the electron densities and temperatures are discussed in Chapter III, section II.

CHAPTER I

CO_2 Molecule and Vibrational Energy Transfer in Pure CO_2

Before considering relaxation processes in gases and experimental measurements, some general knowledge of the CO_2 molecule is needed. An understanding of fluorescence at 4.3μ and how this phenomenon can be used to measure relaxation rates in gases is given in the first part of this chapter, which deals with the CO_2 molecule.

CO_2 Molecule

The CO_2 molecule is a linear, symmetric molecule possessing three fundamental modes of vibration (Ref. I): a symmetric mode designated by (NOO), a degenerate bending mode (ON^1O) (1 represents the angular momentum with respect to the longitudinal axis of the molecule -(1 and N have the same parity and $O \leq 1 \leq N$) and an asymmetric mode (OON). The rotation of the molecule is degenerate and represented by the quantum number J.

The principle transition occurs between the states (001), J=19 and (100), J=20 called the P(20) transition. Therefore, in the cell a molecule in the (100), J=20 state receiving a photon at 10.59μ is going to absorb it and be excited to the (001), J=19 state. Conversely a (001), J=19 molecule will by stimulated emission due to the incident photon, make a transition to the lower level. This phenomenon occurs during a very short time corresponding to the pulse length (in our case typically 1 μsec), after which the level populations slowly relax to their steady state values.

Lower vibrational state radiative lifetimes and transition

ENERGIES AND TRANSITIONS OF THE LOWER CO_2 LEVELS

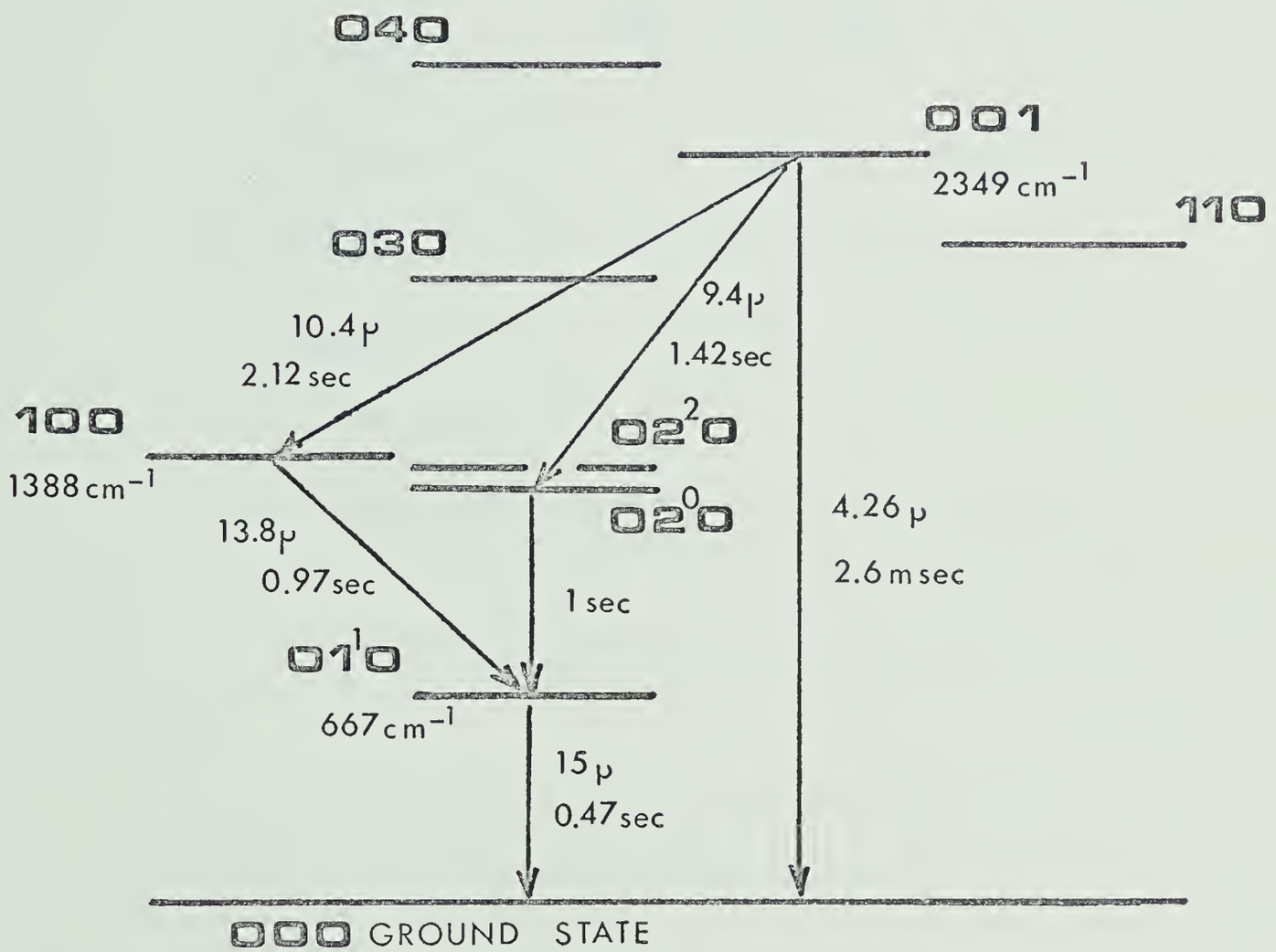

FIG. 11

wavelengths are given in Fig. II, where it can be remarked that the most probable transition from the (001) level is to the ground state by radiation of 4.3μ. This radiation is effectively trapped because of the large absorption constant for this wavelength. See Appendix I for the absorption coefficient and the relation between absorption and the rotational quantum number.

In thermal equilibrium the number density of a state is given by :

$$1 \qquad N_{\nu,J} = N_o \frac{2hcB}{KT}(2J+1)\, e^{\frac{-hcB}{KT}J(J+1)}\, e^{\frac{-E_\nu}{KT}}$$

where $B=0.39\ cm^{-1}$ from Hertzberg (see Fig. II for energy levels). Thus using 1, $N_{(100)}=1.1510^{-3}N_o$; $N_{(100)J=19}=7.10^{-5}N_o$

$$N_{(001)}=1.410^{-5}N_o \quad \text{for } T=293°k$$

Collision Relaxation of the (001) Level :

If the gas was collisionless the return to the thermal equilibrium population by an over populated state would be done radiatively. In our case the radiative lifetime of the 001 level is 2.6msec.

In the presence of collisions some inelastic processes such as

$$2 \qquad \begin{aligned} CO_2(001)+CO_2(000) &\rightarrow CO_2(110)+CO_2(000)+273cm^{-1} \\ &\rightarrow CO_2(030)+CO_2(000)+416cm^{-1} \\ &\rightarrow CO_2(040)+CO_2(000)-204cm^{-1} \end{aligned}$$

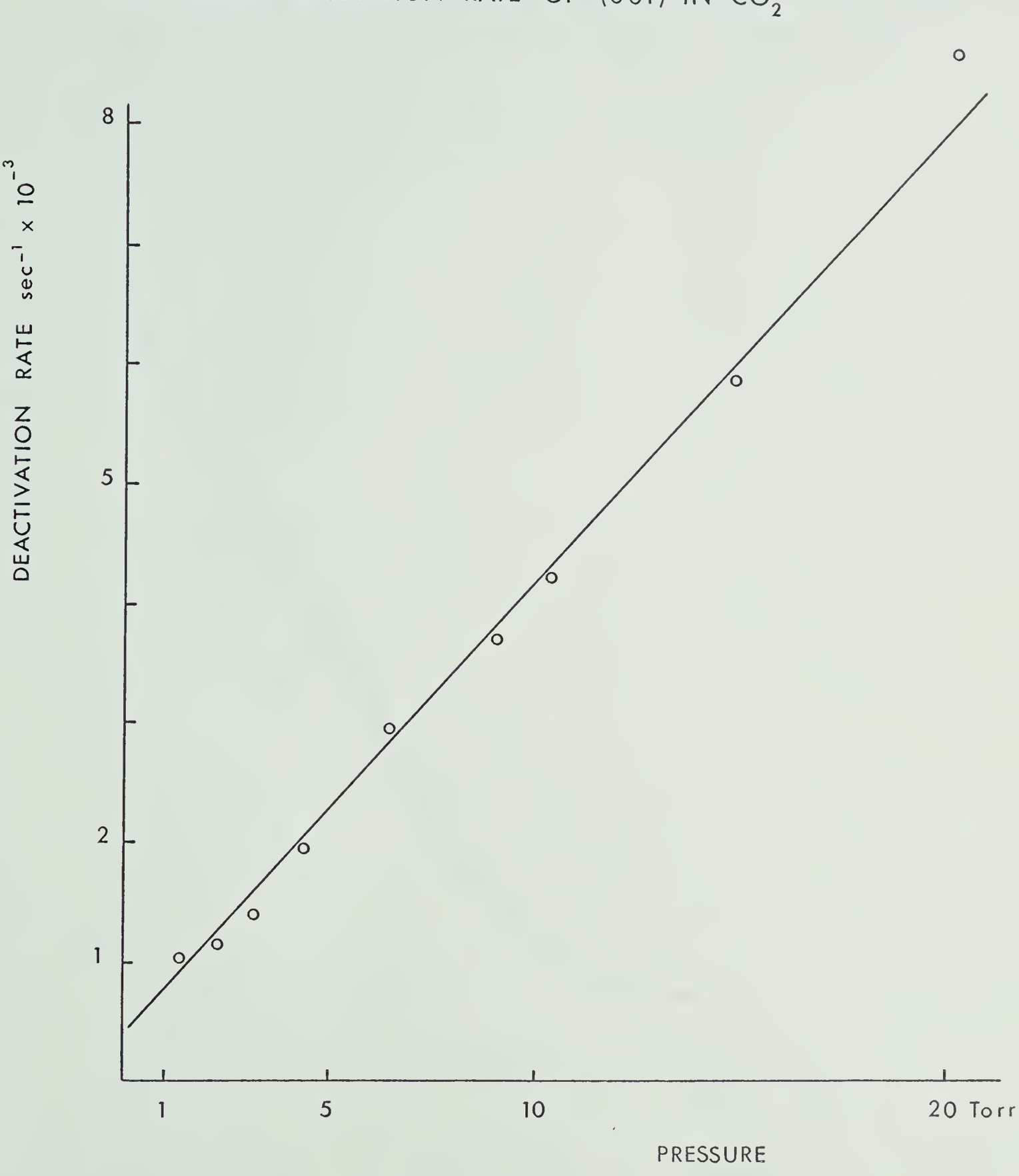
COLLISIONAL RELAXATION RATE OF (001) IN CO_2
DEACTIVATION RATE $sec^{-1} \times 10^{-3}$
8
5
2
1
1
5
10
20 Torr
PRESSURE

FIG. III

TEMPERATURE DEPENDENCE OF THE (001) RELAXATION RATE

(AFTER ROSSER ET AL)

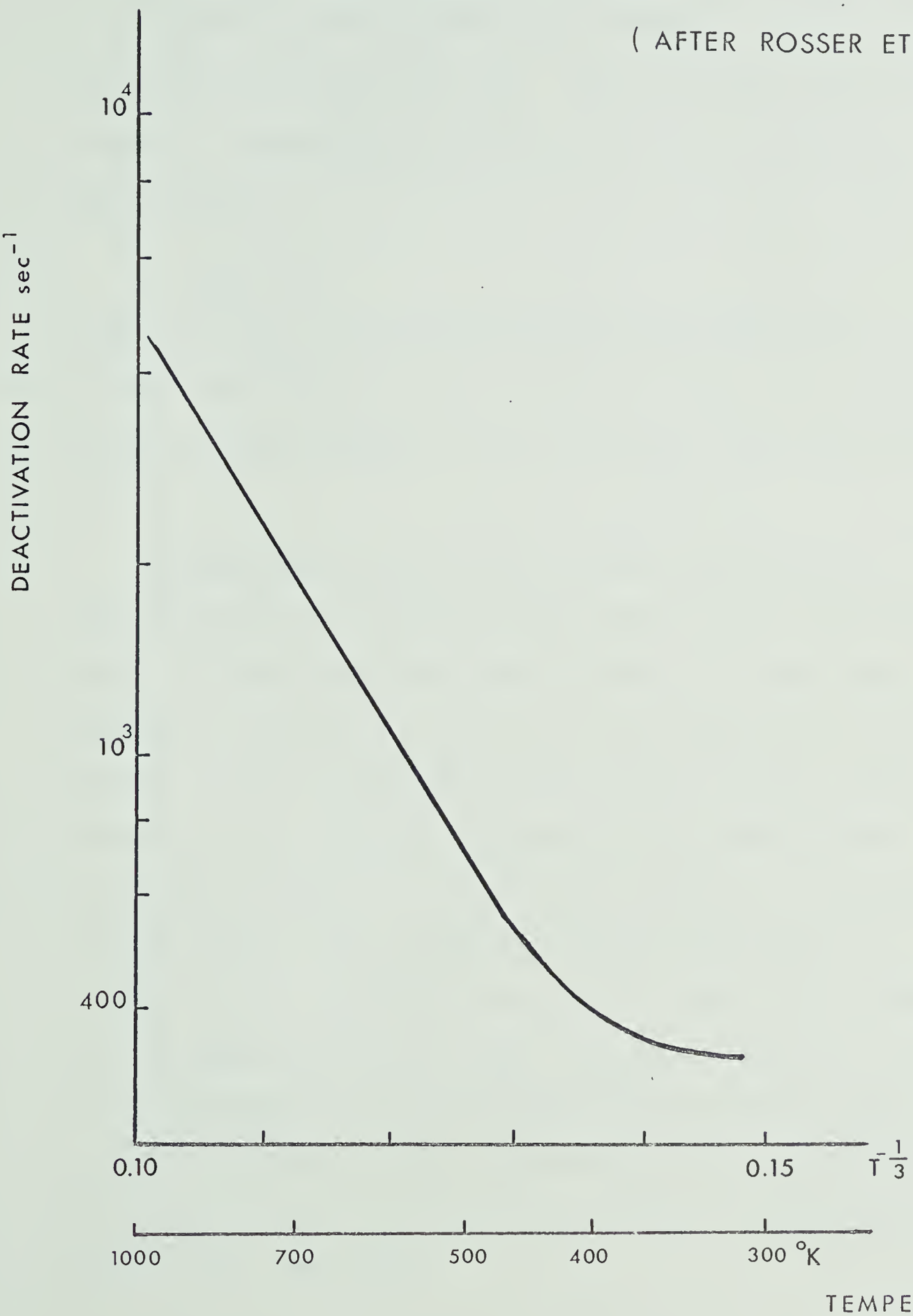

FIG. IV

or, more generally

3 $CO_2(001)+CO_2(000)\rightarrow CO_2(NMO)+CO_2(N'M'O)+\Delta E$

can de-excite the upper laser state. The rate of these collisional processes is proportional to pressure and thus the total rate may be written

4 $k = k_{RAD} + k_c P$

Moore et al found a rate of deactivation for the (001) level of 350 sec^{-1} $torr^{-1}$±10 while Hocker et al found 385±40. More recently Rosser et al have measured at room temperature a rate of 330 sec^{-1} $torr^{-1}$.

Our experiment does not allow a better measurement but it shows that since our less sophisticated apparatus gave comparable results, it may be used with greater confidence in making other measurements (see Fig. III). With our cell, using glass and salt windows, we could not heat the gas high enough to get the temperature dependence of this collisional relaxation rate. This relation was measured by Rosser et al and is shown in Fig. IV. Our measured value of 380 sec^{-1} $torr^{-1}$ agrees with these values within experimental error. A possible reason for the larger value obtained here, as compared to 330 sec^{-1} $torr^{-1}$, may be gas impurity. Anyway our measurement was done in commercially pure CO_2 gas, which is typical of practical lasers. This number is more representative of the CO_2 laser than the 330 sec^{-1} $torr^{-1}$ given for high purity gas and a very clean system.

CHAPTER II

Deactivation of the Upper Level of CO_2 by Different Gases.

Knowledge of the deactivation rate of the (001) level by nitrogen is very important because it is by the inverse process that the CO_2 molecule is efficiently excited to the upper laser level. In addition, (001) deactivation by carbon monoxide has been measured, since the level of CO can be quite high in a sealed-off CO_2 laser.

CO_2-N_2 Inelastic Processes

The diatomic N_2 molecule has no infra-red active transition and the first vibrational level is 2331 cm^{-1} above the ground state and almost energetically matched with the (001) level of CO_2. Some collision phenomena relating to (001) that can occur are:

5 a) $CO_2(001) + N_2(0) \rightarrow CO_2(000) + N_2(1) + 18.6cm^{-1}$

b) $CO_2(001) + N_2(0) \rightarrow CO_2(NMO) + N_2(0) + \Delta E$

c) $CO_2(000) + N_2(1) \rightarrow CO_2(NMO) + N_2(0) + \Delta E$

and the CO_2-CO_2 collision.

3 $CO_2(001) + CO_2(000) \rightarrow CO_2(NMO) + CO_2(N'M'O)$.

The deactivation of nitrogen by vibrational-translational energy exchange is very slow compared with the time scale considered in this experiment (Ref. V).

RELAXATION RATE OF THE (001) BY N_2 AND CO

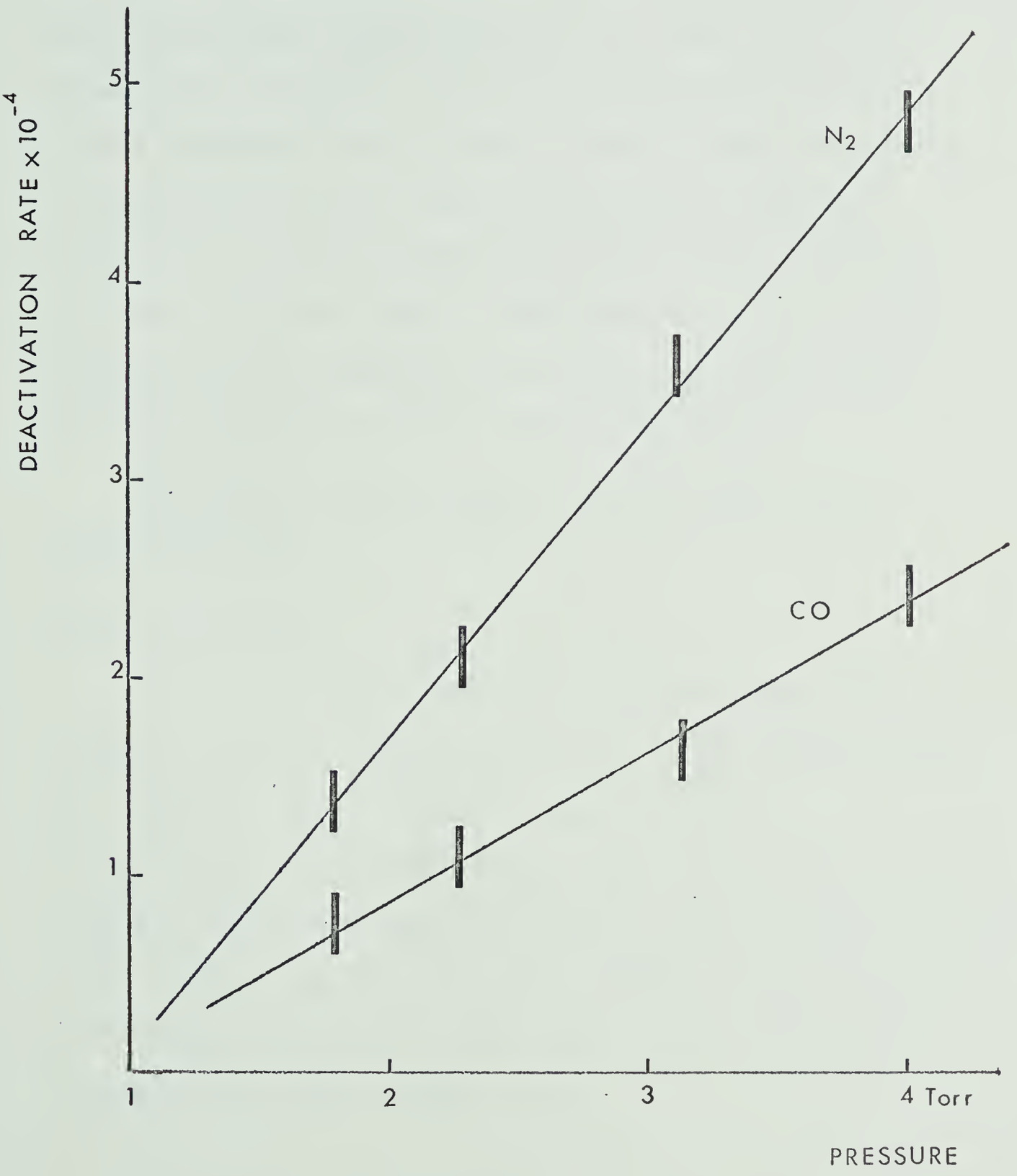

FIG V

It has been shown that the rate of 5a is much faster than any of 3, 5b, 5c. This means the first part of the pulse decay will reflect primarily the reaction 5a resulting in a population equilibrium between $CO_2(001)$ and $N_2(1)$ after which both relax by means of 3, 5b and 5c. The rate of the fast decay measured in this experiment is given in Fig. V versus nitrogen pressure for a CO_2 pressure of 1 torr. The resulting rate is 16 000 sec^{-1} $torr^{-1}$ which is in good agreement with the measurement of Rosser et al and a little less than the 19000 given by Moore et al. The slower rate was not measured because of low signal level, but this rate is known to be smaller than the CO_2-CO_2 one.

Relaxation of (001) by other collision partners may be found in Ref. IV.

CO_2-CO Interaction :

It was surprising to find that a comparable CO_2-CO fast relaxation rate has not been measured before, since: (i) the reaction

5d $\quad CO_2(001) + CO(0) \rightarrow CO_2(000) + CO(1) + 206cm^{-1}$

is near resonant and therefore likely large, and (ii) CO is generally present in significant quantities in the CO_2 laser through dissociation of CO_2. We have measured a fast rate of 8000 $sec^{-1}torr^{-1}$ corresponding to reaction 5d which is indeed large (see Fig. V for the deactivation rate versus pressure of CO).

If we compare the ΔE of 206 cm^{-1} with the 18.6 cm^{-1} of the nitrogen reaction the level of CO seems to be too far away from

the resonance to get a rate of deactivation as high as half of the nitrogen's one. Sharma and Brau (Ref. XII) have given a explanation for the behaviour of the N_2-CO_2 inelastic process using a "dipole-quadrupole" interaction potential. Using this model, they have predicted the temperature dependence of the relaxation rate measured by Rosser et al (Ref. XIV).

It would be interesting to know the dependence of the CO_2-CO collision rate on temperature, for with such information we would be able to determine the interaction potential involved in this case. A suggestion for the proper calculation is that the "dipole-quadrupole" interaction of CO_2-N_2 should be replaced by a "dipole-dipole" interaction, the 2143cm^{-1} level of CO being infra-red active and the CO molecule having a permanent dipole moment.

CHAPTER III

CO_2 - Electron Inelastic Processes.

This chapter deals with the effect of a glow discharge on molecular population and relaxtion rates. It is composed of four sections :(i) a discussion from the previous work of Hake and Phelps, and Boness and Schulz on the excitation rate of the different levels of the CO_2 molecule, (ii) measurements of the discharge parameters, electron densities and energies, temperature of the gas and carbon monoxide level, (iii) the influence of the discharge on the level of the 4.3μ fluorescent signal, which is related to population inversion and (iv) the deactivation rate of the (001) state as a function of electron density. In an appendix to this chapter a calculation is made of the electron - CO_2 excitation and de-excitation rates for the (001) level.

CO_2 Excitation.

Some electron excitation cross-sections have been obtained from double electrostatic analyser measurements in CO_2 (Ref. VII and VIII); they are shown in Fig. VI. With these results we can get some idea of how the electrons are likely to affect relaxation and excitation processes in our experiment. Later, in section (iv), we shall present experimentally measured electron -CO_2 relaxation rates.

1 Direct excitation of the symmetric mode (100).

The reaction considered here is

6 $$CO_2(000) + e \rightarrow CO_2(100) + e - \Delta E = 0.17 \text{ ev}$$

EXCITATION CROSS-SECTIONS OF CO_2 LEVELS BY ELECTRONS

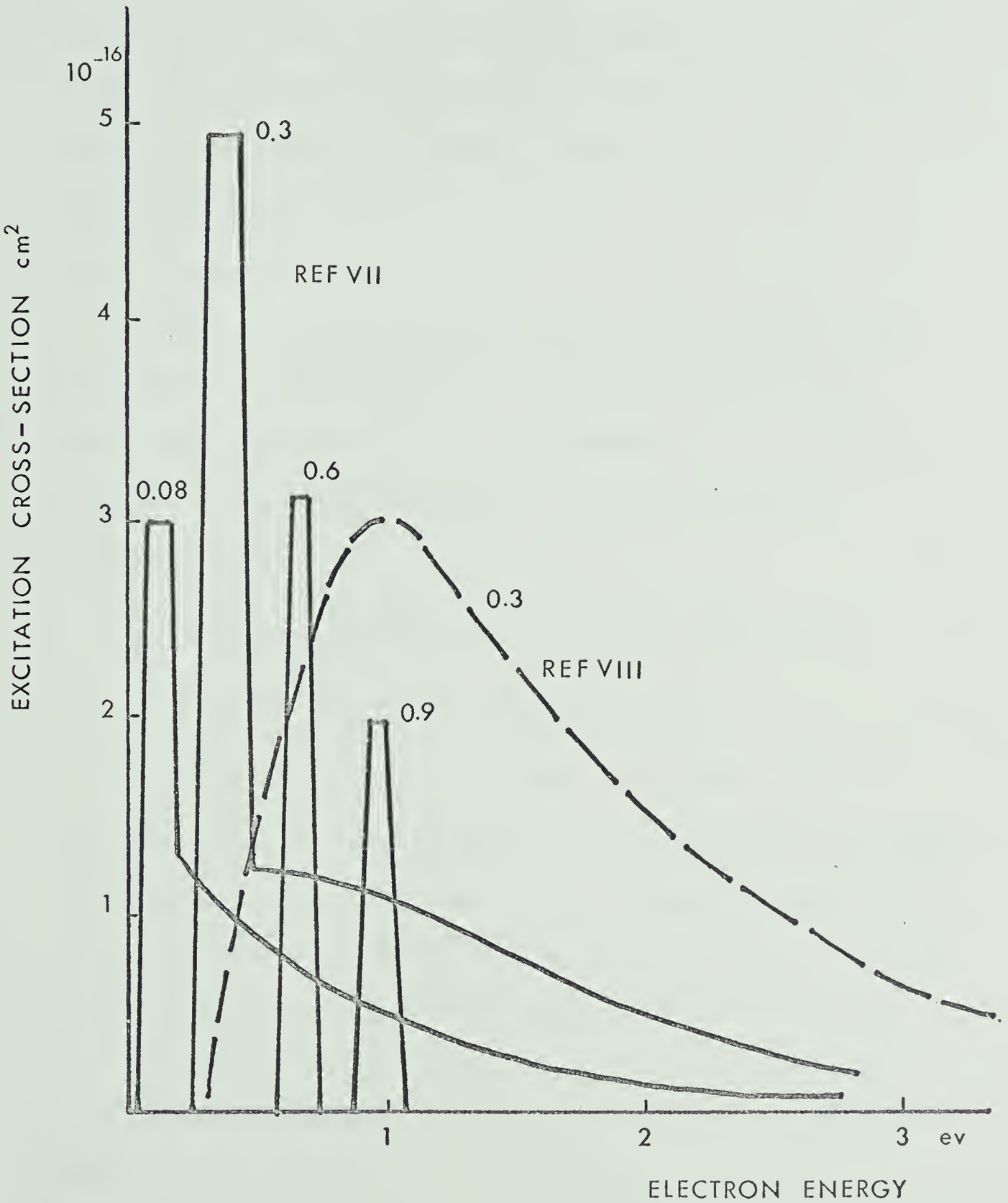

FIG.VI

This cross-section is small compared with other inelastic processes in CO_2 and with the elastic cross-section of $10^{-15}cm^2$ (Ref. VIII). If we assume a value of $210^{-17}cm^2$, which seems to be an upper limit, for typical CO_2 discharge conditions (2 ev, 10^9 electrons/cm^3) we get an excitation rate of 2 sec^{-1}. This rate is too small to change the (001) population in any significant manner.

2 Bending mode.

We are not directly interested in the (ONO) mode but the strong Fermi resonance between the (100) and (02°0) levels means that a change in vibrational temperature in the bending mode affects the (100) population. Thus (100) excitation could proceed via

7 a. $CO_2(000) + e \rightarrow CO_2(010) + e - 0.08$ ev (667 cm^{-1})

b. $2CO_2(010) \rightarrow CO_2(000) + CO_2(02°0) + \Delta E$

c. $CO_2(020) + CO_2(000) \rightarrow CO_2(100) + CO_2(000) - 102\ cm^{-1}$

The cross-section of reaction 2a has been given by Hake and Phelps in the 0.08 ev region (Fig. VI). If we assume a 2 ev Maxwellian distribution for the electrons only a few percent of the electrons are in the resonant cross-section region. The calculated rate for 2a is found to be only 2 sec^{-1} still too small to affect the (100) population even with infinitely fast relaxation between (ONO) and (100). These results mean that the population of the (100) level is going to be governed principally by the temperature of the gas (see App. II and Fig. XIV).

3 Excitation and de-excitation of the asymmetric mode (001).

Before any cross-section measurements were made, inelastic excitation of the (001) was known to be efficient enough to create an inversion of population between the (001) and the (100) levels (without nitrogen present).

This cross-section has been obtained by Hake and Phelps (Ref. VII) and by Boness and Schulz (Ref. VIII). Their results are quite different and in the next part we are going to use the recent work of Boness and Schulz. The reaction considered here is given by

8 a. $CO_2(000) + e \rightarrow CO_2(00N) + e + N \times 0.3$ ev

The inverse process of deactivation of (00N) state

b. $CO_2(00N) + e \rightarrow CO_2(NMO) + e + \Delta E$

is going to interest us in the next part of the experiment as well as the excitation of 8a.

Apart from the experimental approach of section iii and iv a theoretical calculation has been performed (see App III). The excitation cross-section computed shows good agreement with the measured one by Boness and Schulz. The de-excitation has never been measured, but this calculation may give some idea of the relative cross-section between excitation and de-excitation processes.

Before proceeding to the experimental results, we pause to consider the gas discharge parameters, chiefly electron density and temperature, and gas temperature.

DISCHARGE VOLTAGE (OVER 7 cm)

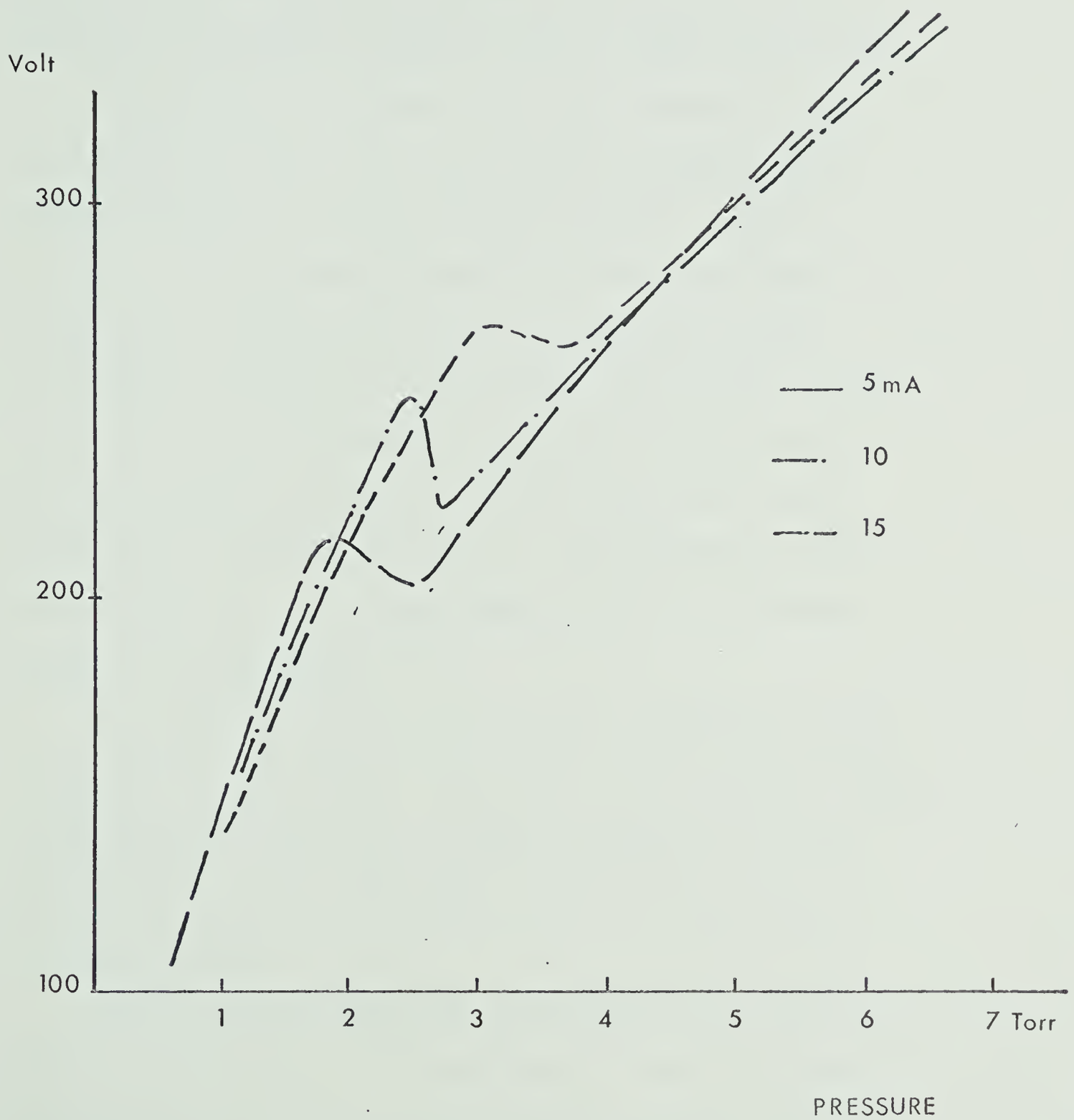

FIG. VII

Measurements of the Parameters in the Discharge.

The electron density and energy were obtained two ways from knowledge of E/P in the discharge and the use of tables given in Ref. XV and by direct probe measurements. The variable E was known from the voltage measured across 7 cm of discharge, and is shown in Fig. VII versus current and pressure.

The two straight portions of the curve between 0.75 torr and 2 torr and between 3 torr and 7 torr were reproducible to within a few percent but the transition around 2.5 torr was unstable. In this pressure range from 2-3 torr the voltage always showed a maximum and minimum, sometimes two occured. It can also be noticed that the two slopes in the linear portion of the curve are quite different suggesting there may be two different inelastic processes in the discharge having a sharp transition at a pressure of 2.5 torr. This phenomenon is going to be discussed later on in this chapter since the fluorescent signal is strongly related to it.

The calculated electron density N_e and energy T_e are given in Fig. VIII versus pressure. The effect of the discharge current on the potential being small, we assume a density of electrons proportional to current (the density curve is given for 1 ma discharge current).

We have also measured N_e and T_e directly using single and double probe techniques. The densities were determined using a formula given in Ref. XVI for the high pressure region (1-5 torr)

ELECTRON TEMPERATURES AND DENSITIES IN THE DISCHARGE

ENERGY X DENSITY o

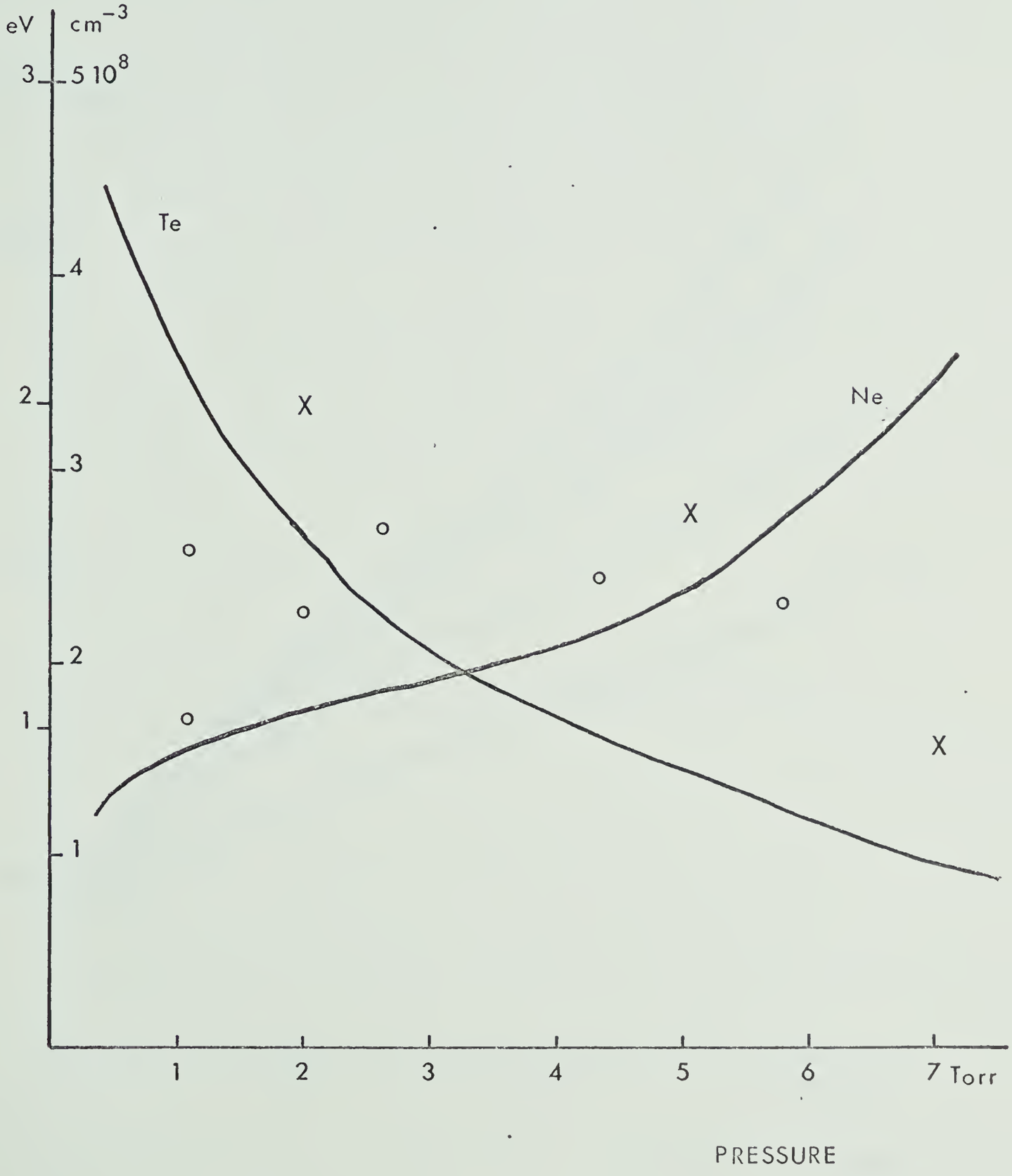

FIG. VIII

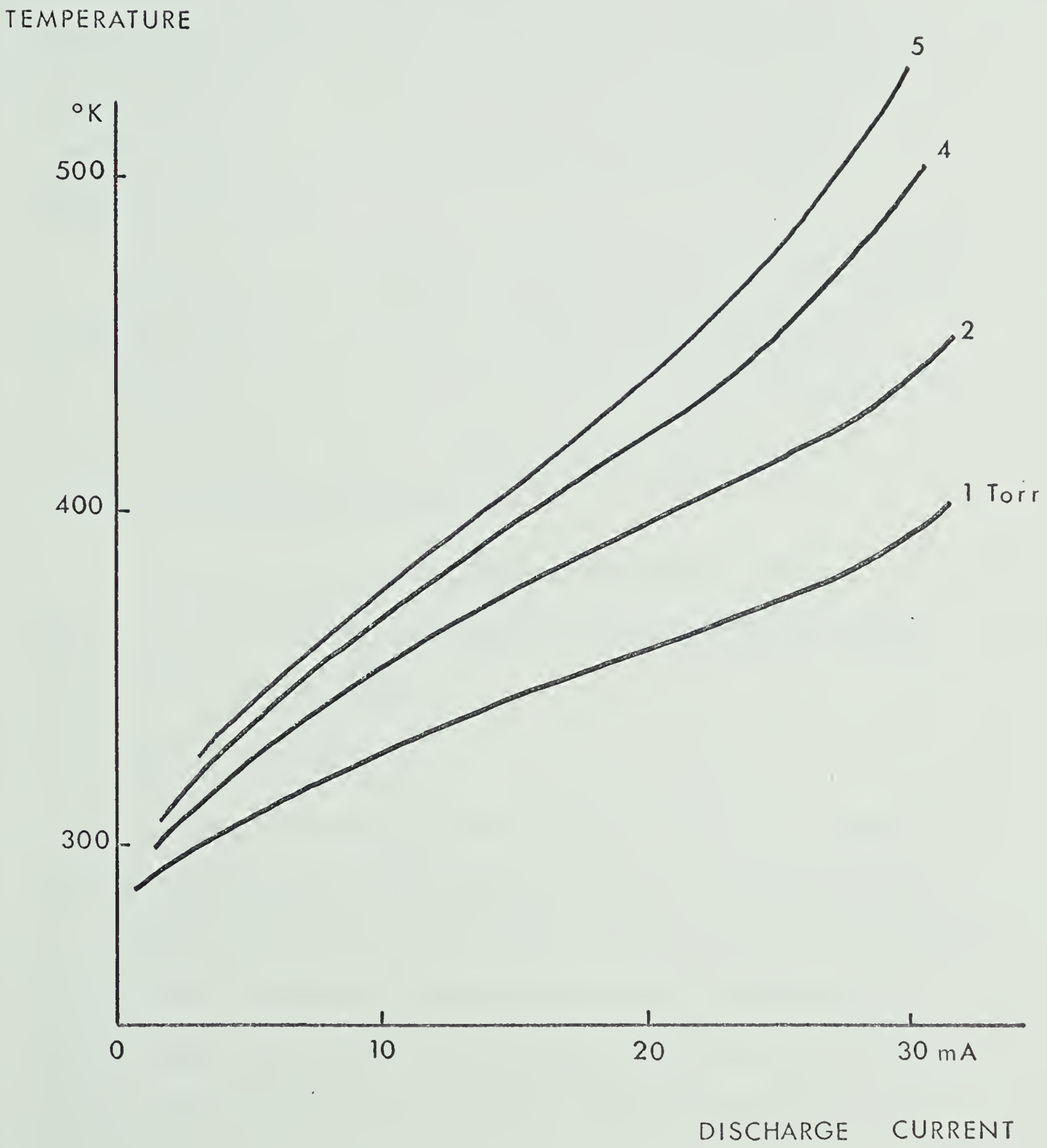
TEMPERATURE
°K
500
400
300
5
4
2
1 Torr
0
10
20
30 mA
DISCHARGE CURRENT

FIG. IX

from current collected versus probe voltage. The energies were calculated from slope measurements at the zero point of current-voltage curves. These results are shown in Fig. VIII as dots. They are quite different from the ones obtained from E/P. The principal reason is presumably due to the imprecision in the probe technique itself; in our case gas and probe impurities may also be responsible. Qualitative and semi-qualitative agreement is adequate which justifies using these values for order of magnitude calculations.

Knowledge of the temperature of the gas is important because of the large effect it has on the CO_2-CO_2 de-activation rate (Fig. IV)(Ref. V). This measurement was done using a thermocouple in front of the side windows and is shown in Fig. IX versus pressure and discharge current.

It is known that a CO_2 discharge can produce a large amount of CO from direct decomposition of CO_2 by electron impact under the following process:

9 $\quad CO_2 + e \rightarrow CO + \underline{O} + e$

We have previously measured the de-activation rate of the upper level by CO and found it to be very efficient. Therefore if we want to measure the de-activation rate depending only on the electron action we have to know the CO proportion in the discharge. We did not expect this level to be very high since the gas is flowing and the viewing window is only a few cm from the beginning of the discharge.

An analysis of the discharge gas products was done using a Perkin-Elmer 421 spectrophotometer and it showed that the level of CO in the most unfavourable case is only 2% (60ma current). The level of CO is going to be smaller at lower current (where most experimental measurements were made) and indeed its effect is small compared with the electron one as we shall see.

Inversion in Population Between the (001) and (100) Levels.

The results to be discussed in this section and the following one are based on the fluorescent technique described earlier.

In thermal equilibrium the population of the different levels is given by equation 1

$$N_{\nu,J} = N_o \frac{2hcB}{KT} (2J+1) e^{-\frac{hcB}{KT} J(J+1)} e^{-\frac{E\nu}{KT}}$$

N(100) is then larger than N(001).

In some cases an inversion of population can be built up by direct excitation, by transfer from vibrationally excited nitrogen or by other processes. Let us see how this inversion phenomenon is going to influence the fluorescent signal at 4.3μ.

In thermal equilibrium and before the laser pulse N(001)<N(100) for a non-discharge case. During the pulse time the population of the upper level is increased by a certain number of the order of N(100). This extra population is going to relax by means of collisions or relaxative transitions to the equilibrium number of molecules N(001). It means we will see at the time of pulse a sudden increase in fluorescence followed by an exponential decrease

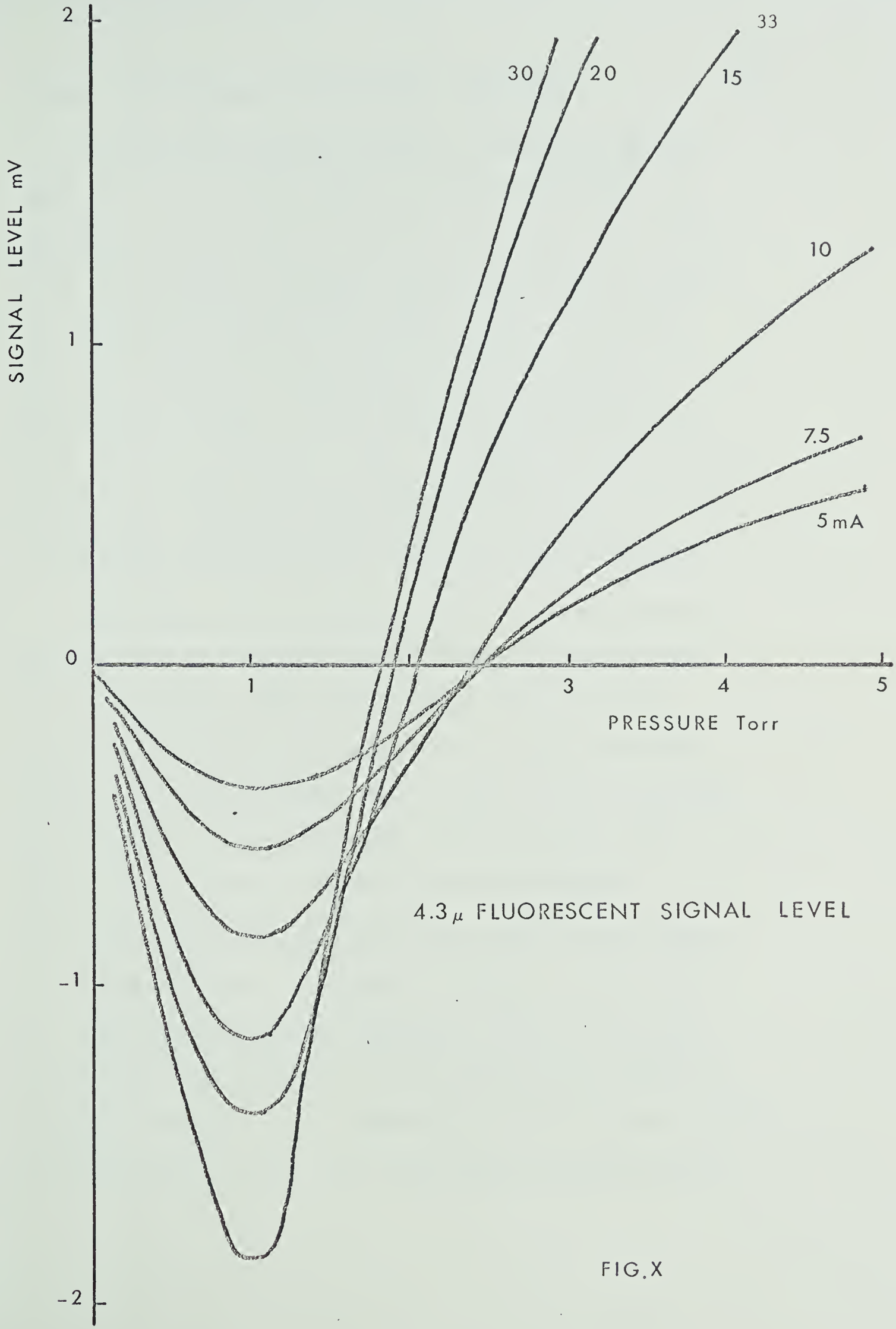
2
1
0
-1
-2
SIGNAL LEVEL mV
33
30
20
15
10
7.5
5 mA
1
3
4
5
PRESSURE Torr
4.3 μ FLUORESCENT SIGNAL LEVEL

FIG. X

showing the collisional and radiative decay rate.

On the other hand when inversion is created before the laser pulse the population N(001) is larger than N(100). In this case during the pulse the number of molecules in the (001) state is decreased by stimulated enversion and after the pulse the "equilibrium" population is built up again by collisions from other levels, and by excitation from the ground state. The fluorescent signal at 4.3μ is going to decrease during the pulse and increase after it. These two different effects of 10.6μ emission and absorption corresponding to a decrease or increase in the (001) population are the subject of the next paragraph.

The level of the fluorescent signal at 4.3μ was directly measured on an oscilloscope or was recorded on polaroid film for later analysis. This level is given in Fig. X versus pressure, and the different curves are for constant discharge current. The negative values of 4.3μ signal are for a decrease and the positive for an increase in the fluorescence. From Fig. X., three different regions can be distinguished:

(i) the first region between 0 and 2 torr where all the curves are of negative signal, which means a discharge current as low as 2.5 ma built up inversion between the (001) and the (100) levels (note: the maximum signal and therefore the maximum inversion is created at 1 torr independent of the discharge current),

(ii) a transition region, 1.9-2.5 torr, where inversion may or

may not occur depending on the discharge current, and (iii) a third high pressure region where inversion never appears. Let us examine these three different processes in detail.

Low pressure region.

First consider the 1 torr region which is the typical case of the low pressure electrically excited CO_2 laser. Fig. XI gives the level of the signal versus current at constant pressure, for pressure lower than 1.8 torr. These curves all start in the positive region since when no discharge is present there is no inversion. The lower portion of the curves are extrapolated to the non-discharge condition which is experimentally known; the data for the 0-2 ma region were not obtained because the current was too small to sustain a discharge in our apparatus. This extrapolation gives us the point of intersection between the curves and the horizontal axis, where we can assume the two levels are equally populated. It should be remarked that since the relation between signal level and number of radiating molecules is only roughly known (see App I), the intersection point is the most reliable for calculation of vibrational temperature and different excitation parameters.

Interpretation of this transition from absorption to emission of 10.6μ radiation, along with a corresponding increase or decrease in 4.3μ spontaneous emission enables a novel calculation of vibrational excitation in CO_2. We shall show that our results

SIGNAL LEVEL AT LOW PRESSURE

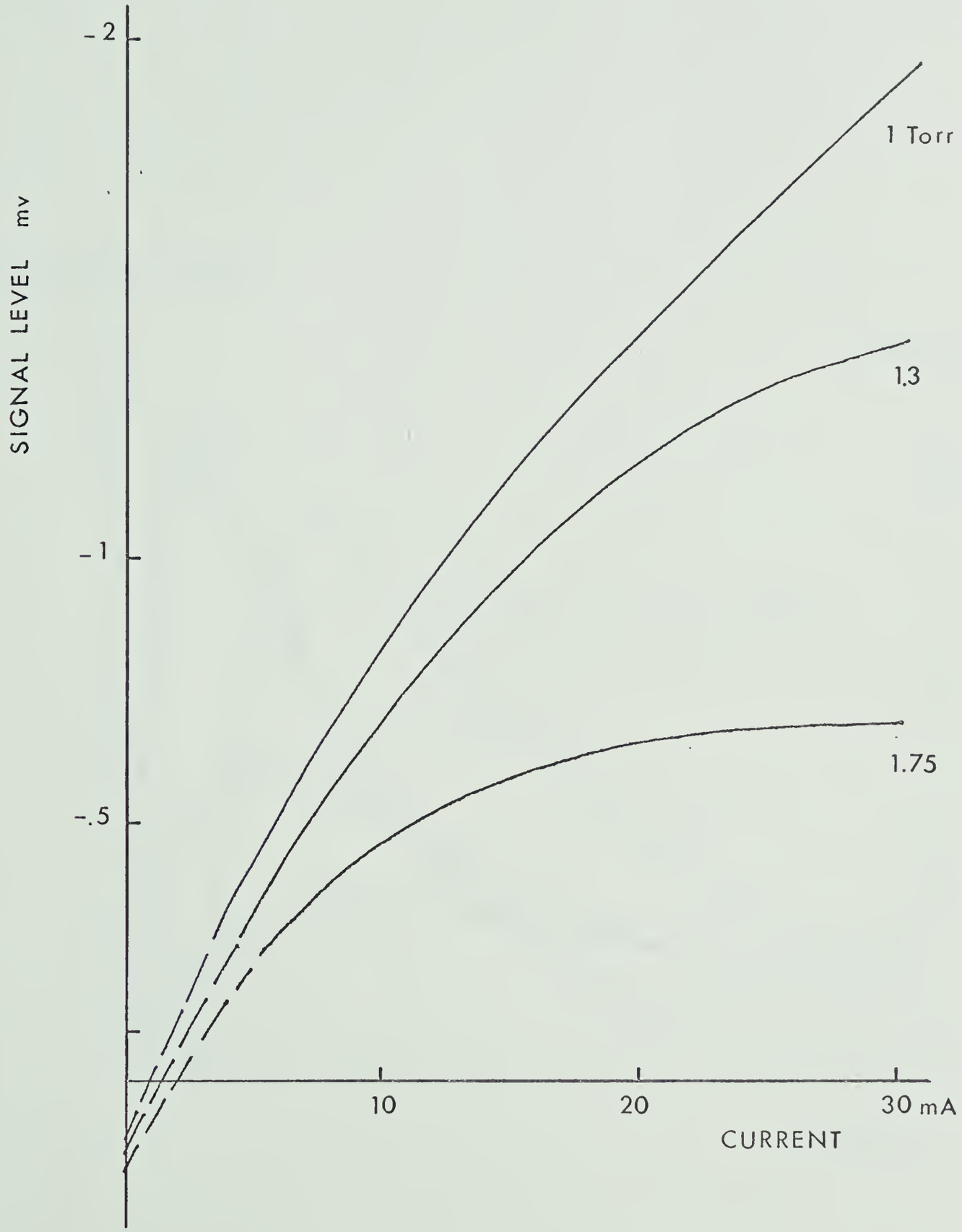

FIG. XI

MAXWELLIAN DISTRIBUTION FUNCTION FOR ELECTRONS

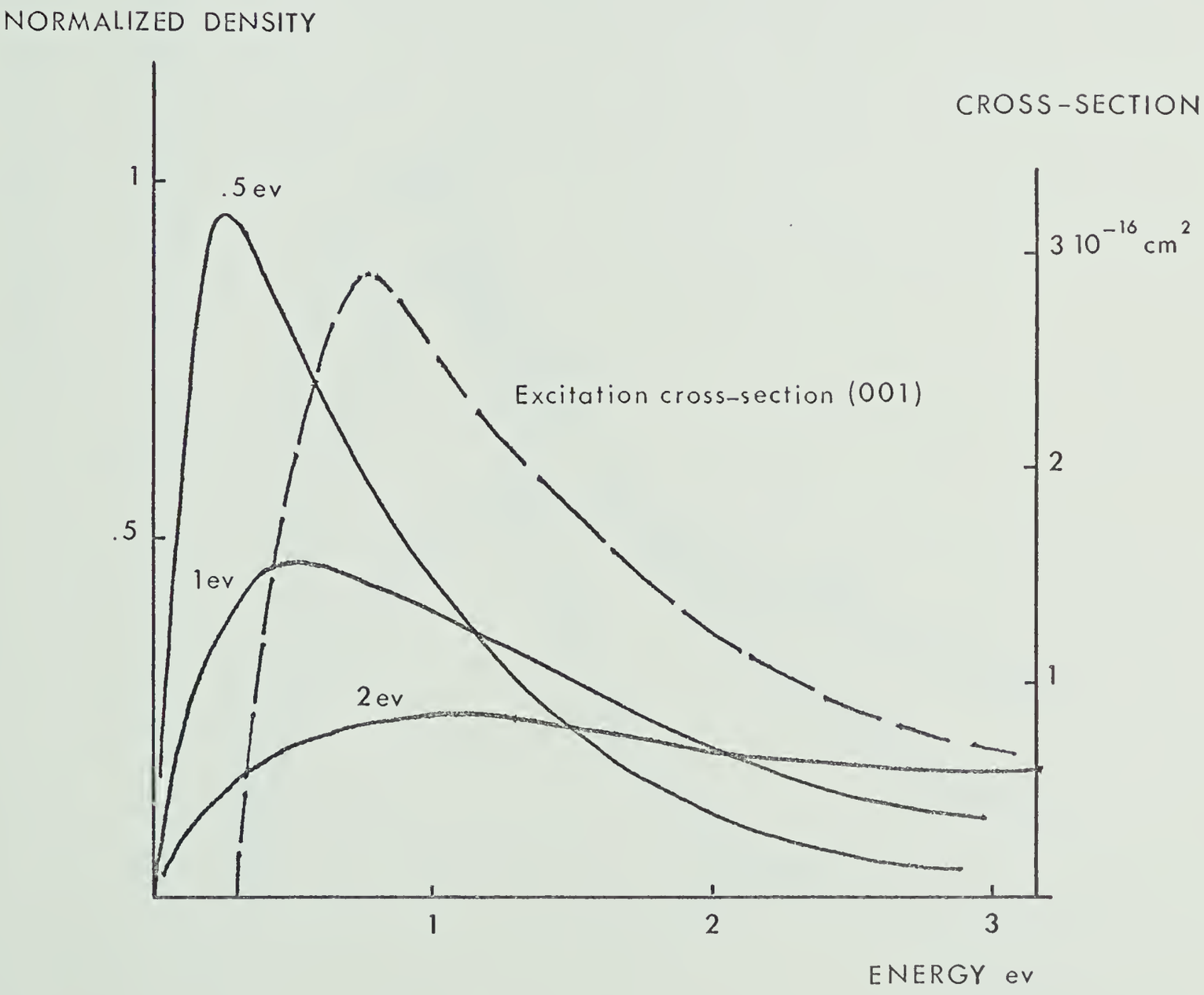

FIG. XII

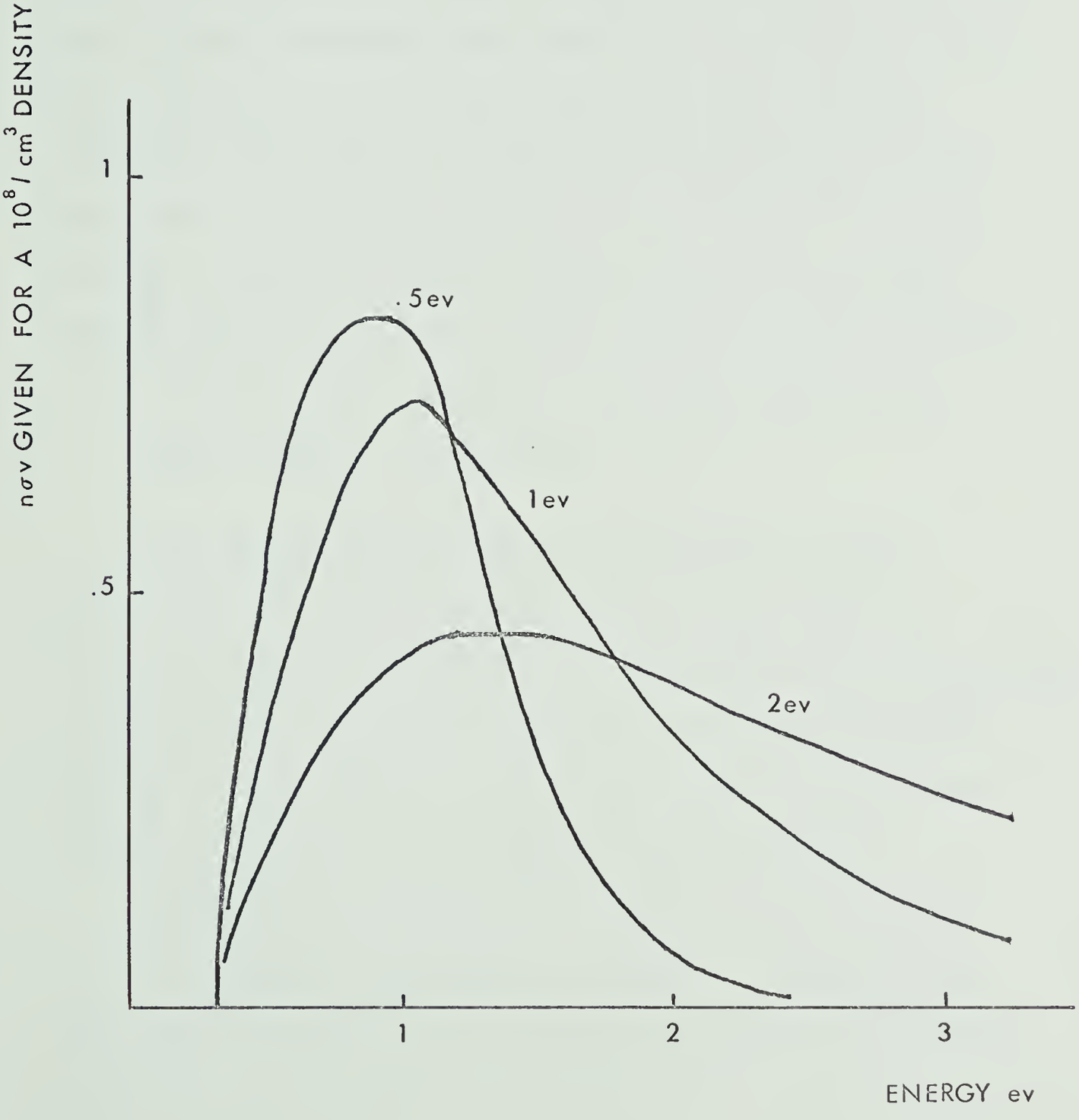
EXCITATION RATE nσv
nσv GIVEN FOR A 10^8/ cm^3 DENSITY
1
.5
.5ev
1ev
2ev
1
2
3
ENERGY ev

FIG. XIII

fit with earlier cross-section measurements and rates of deactivation for CO_2 molecules. We consider the specific case of p = 1 torr in what follows.

The intersection point occur at 1 ma where the density from Fig. VIII is equal to 1.5 $10^8/cm^3$ and the energy is 2 ev. Fig. XII gives different Maxwellian energy distributions and the excitation cross-section for the (001) level (see Ref. VIII). Graphical integration (Fig. XIII) of $n\sigma v$ over all energies gives the total rate, which for the above conditions is $k_e = 1.5\ sec^{-1}$. We have measured in chapter I a total de-activation rate for the (001) level of 800 sec^{-1} at 1 torr; with this number we can now calculate the equilibrium number of molecules in the upper lasing level.

$$N(001) = \frac{1.5}{800}\ N_o = 1.85\ 10^{-3}\ N_o$$

This value is larger, though not by much, than the room temperature population of the (100) lower level ($1.1510^{-3}\ N_o$). Two explanations may be proposed : (i) imprecision in the determination of the excitation rate of the (001) state or (ii) the vibrational temperature of the symmetric mode is higher than the translational temperature of the gas which is 300°K is these conditions.

Assuming the calculation above is representative of an increase in vibrational temperature, the number of molecules in the (100) state is $1.85\ 10^{-3}\ N_o$. The temperature deduced from equation 1 is 315°K. We can suppose because of the Fermi resonance between (02°0) and (100) levels that the vibrational temperature of the symmetric and bending modes are roughly equal. The population of the (010) level is in this case $510^{-2}\ N_o$, versus $410^{-2}\ N_o$ at

room temperature. Now the rate of de-activation of the lower state in the bending mode is known to be 220 sec^{-1} at 1 torr and 300°K; which gives a rate of transfer of energy from the ground state to the (010) level of 2 sec^{-1}. This number can be compared with the 1.5 sec^{-1} rate of population of the (001) level. We know from 2a,b,c and 3 that the de-activation of the (001) level overpopulates the bending mode. The 0.5 sec^{-1} left over can be attributed to direct excitation from ground state to the (010) which in view of Fig. VI is not unrealistic. In conclusion, the experiment gives numbers comparable with the computed ones from known cross-sections.

Transition region.

In a small interval of pressure around 2 torr the inversion may or may not occur depending on the discharge current. We will try to give some explanation for this sharp transition and try to relate it to the one seen previously in the voltage measured across the discharge (see Fig. VII). This voltage transition at 2.5 torr is not accompanied by a significant change in the average electron energy (see Fig. VIII) but it does not mean that the distribution which we have assumed before to be Maxwellian (which is only approximately correct) is not greatly perturbed in this region.

For example, if the pressure is such that an electron energy gain in a collisional mean free path were to equal the excitation energy, a resonance could lead to a local perturbation in the electron energy distribution. We have seen (Fig. VIII)

that the average electron energy decreases with pressure and it is possible that these two effects, perturbation in the distribution and lowering of the average energy, transfer a number of electrons from the (001) resonant excitation cross-section to that of the (010) which would result in loss of population inversion. A detailed investigation of the transition region is clearly required to sort out processes important to loss of inversion.

High pressure case :

Where as in the preceeding cases the signal is governed by electron excitation, here, the gas temperature seems to be a good explanation for the signal behaviour.

When the pressure is higher than 2.5 torr the fluorescent signal is always in the positive region (see Fig. X) which implies that no inversion occurs in the discharge and $N(001)<N(100)$. The signal level is shown for 4 torr in Fig. XIV versus discharge current. The second curve is the signal computed from the translational temperature dependance shown in Fig. IX (see App II), assuming the population of the (100) level is affected only by temperature and the population of the (001) level remained small compared to N(100) for any current. Theoretical and experimental curves are close enough to support the temperature interpretation for the behaviour of the fluorescent signal.

4.3 μ FLUORESCENT SIGNAL LEVEL AT HIGH PRESSURE

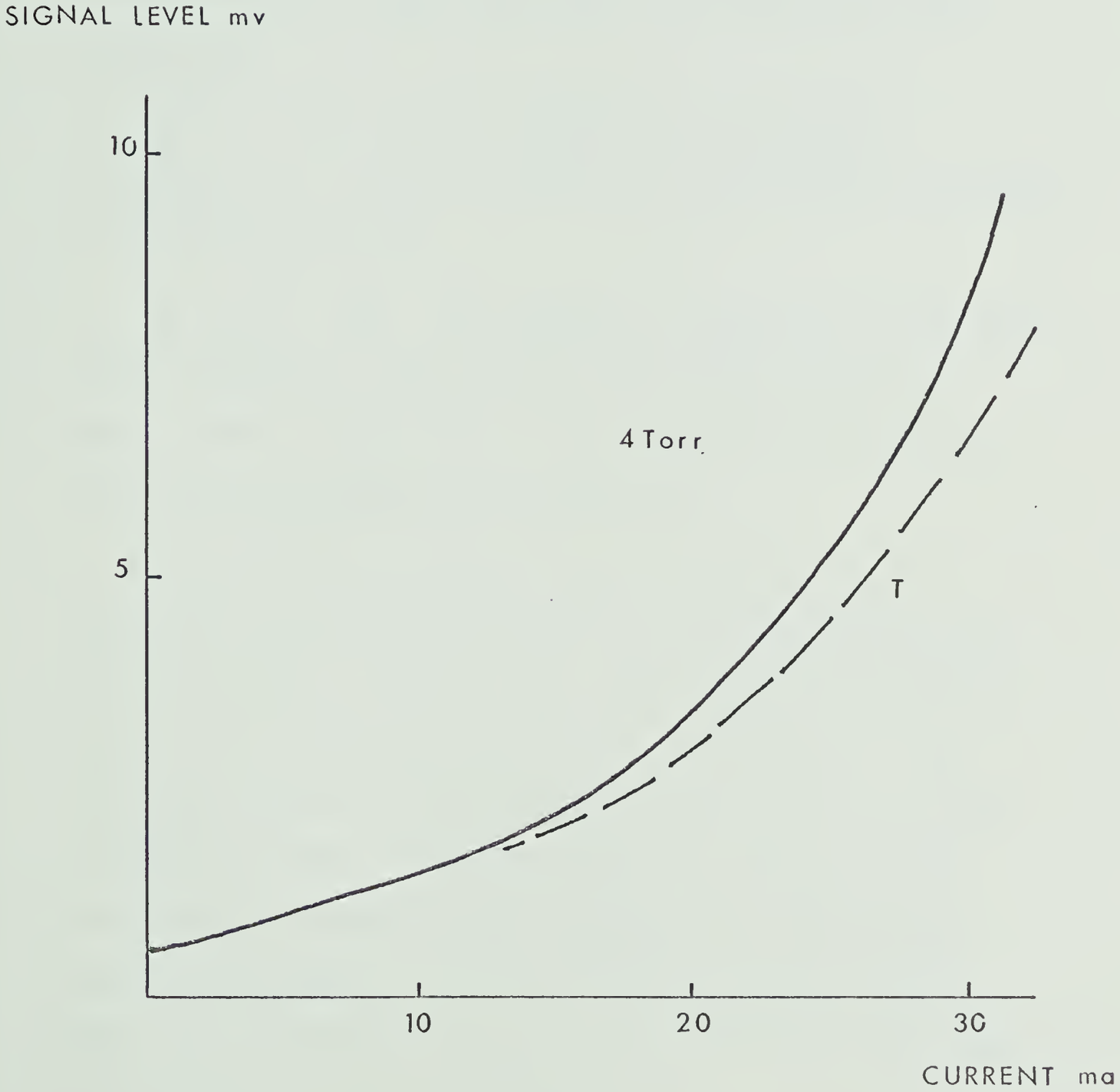

FIG. XIV

Rate of (001) Deactivation in a Discharge.

Not only was the level of the signal measured, but also the decay time of the exponential recovery. We are going to consider the effect of electrons on this time constant and see that it is quite significant. Let us call R the volume rate of population of the upper level and k' the deactivation rate. We can write

10 $\frac{dN}{dt} = R - k'N^*$ where $N^* = N(001)$ and we assume that the pumping rate of (001) is constant for fixed discharge conditions. By integrating 10 we get

11 $N^* = \lambda e^{-k't} + \frac{R}{k'}$. The constant of integration λ is positive when N^* $(t=0) > N^*$ eq., which is the case at high pressure, and negative when N^* $(t=0) < N^*$ eq. at low pressure, but in both cases the exponential recovery rate is given by k'.

The experimentally measured CO_2 deactivation rates for electrons are given in Fig. XV where it can be remarked that all the curves present a positive slope. The temperature compensated curves obtained from Fig. IV and Fig. IX are also shown. From the slope of these curves the increase in rate per ma of current is deduced and shown in Fig. XVI. This last curve shows three different parts comparable to the behaviour of the fluorescent signal versus pressure : a first part with a constant rate of 30/ma. sec a transition at 2.25 torr and a increasing linear part with a rate of the order of 100/ma. sec.

DEACTIVATION OF THE UPPER LEVEL IN A DISCHARGE

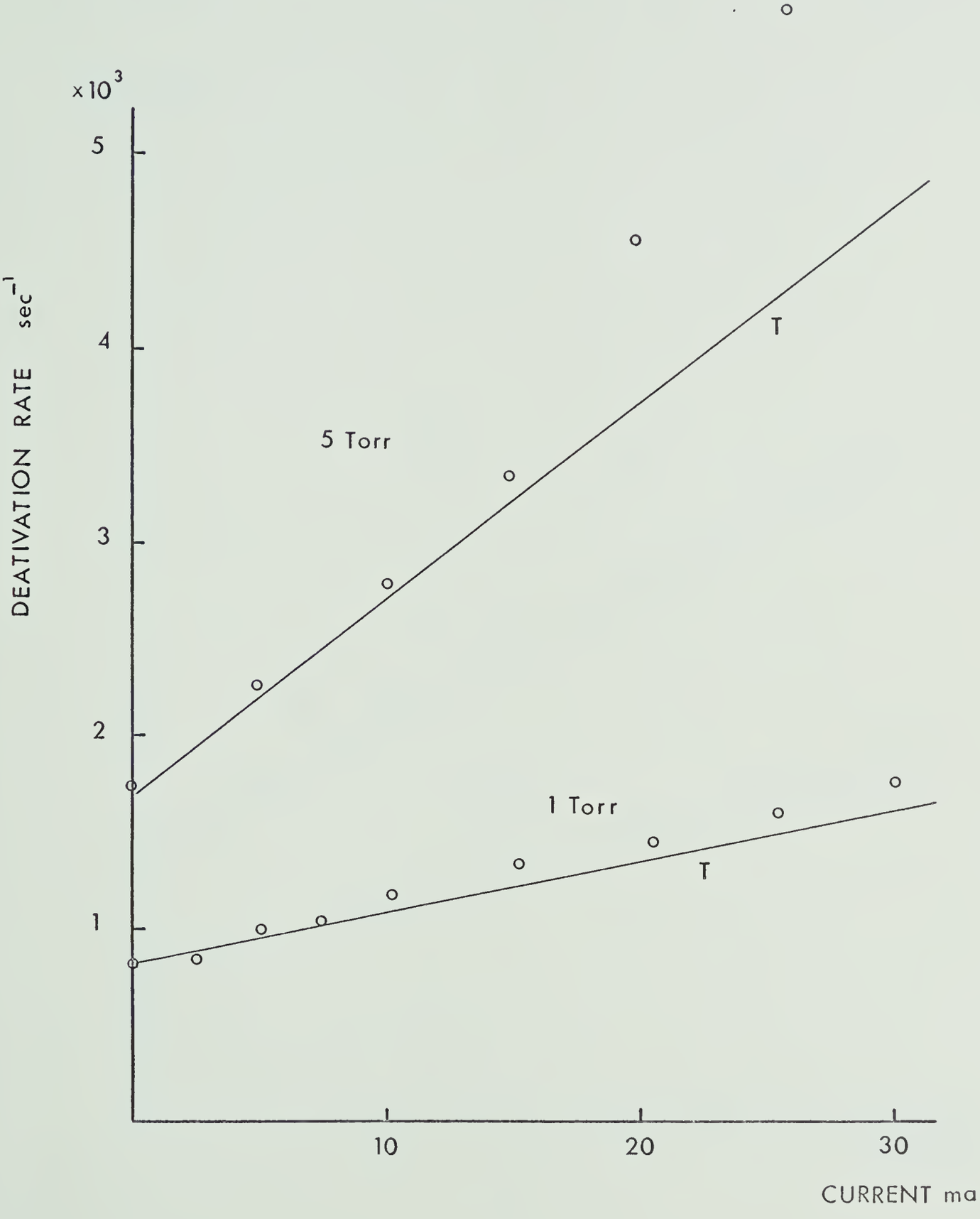

FIG.XV a

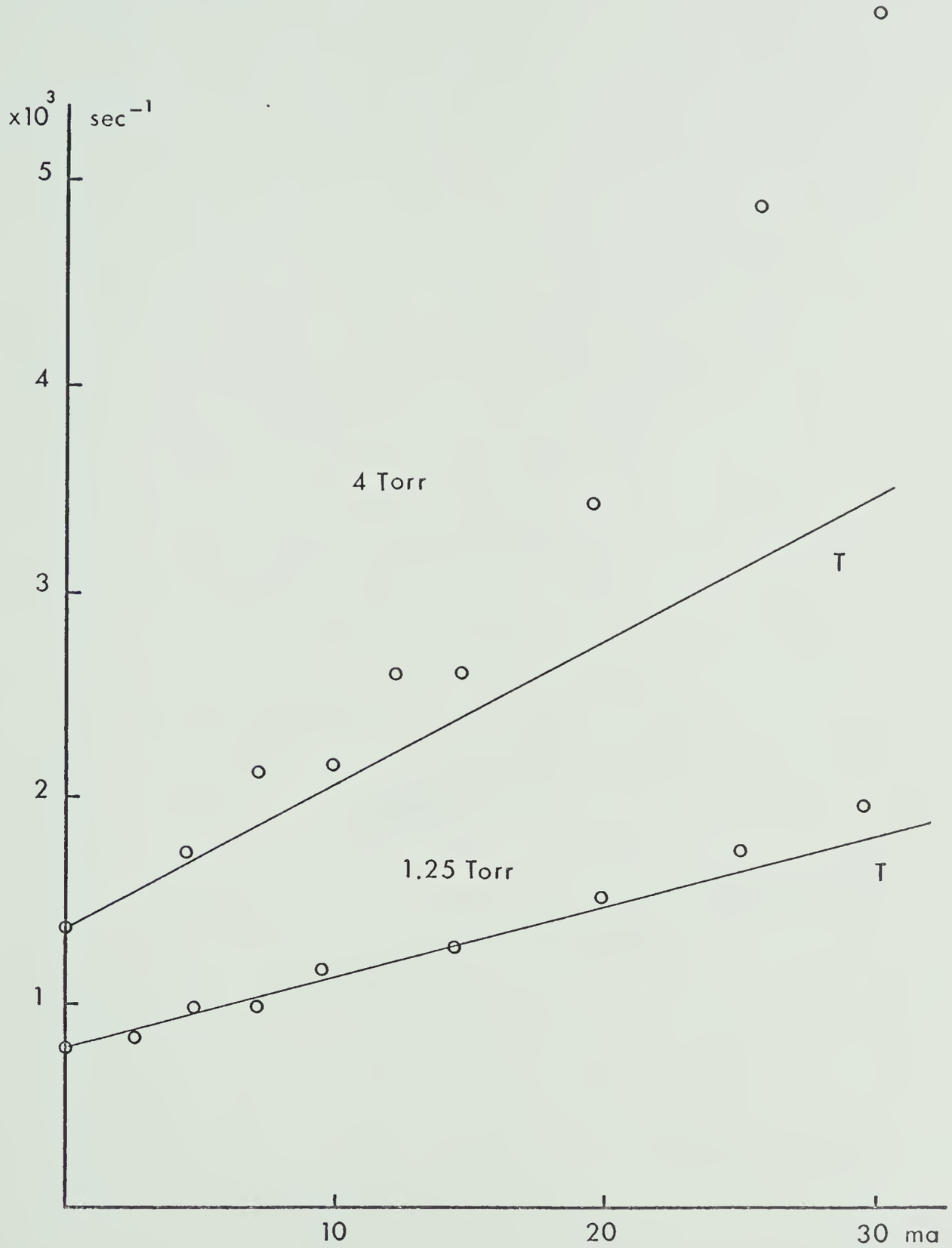

b

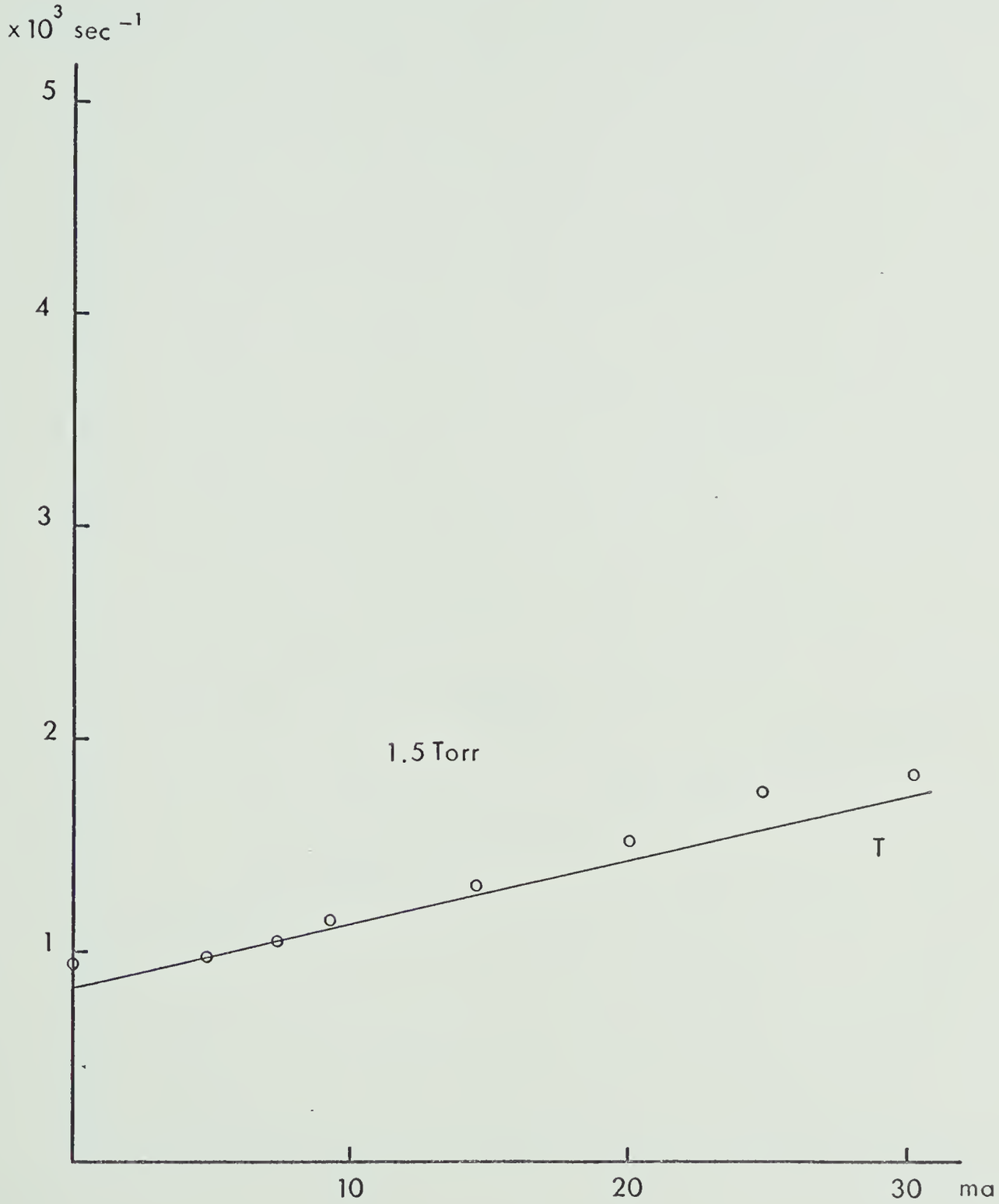

c

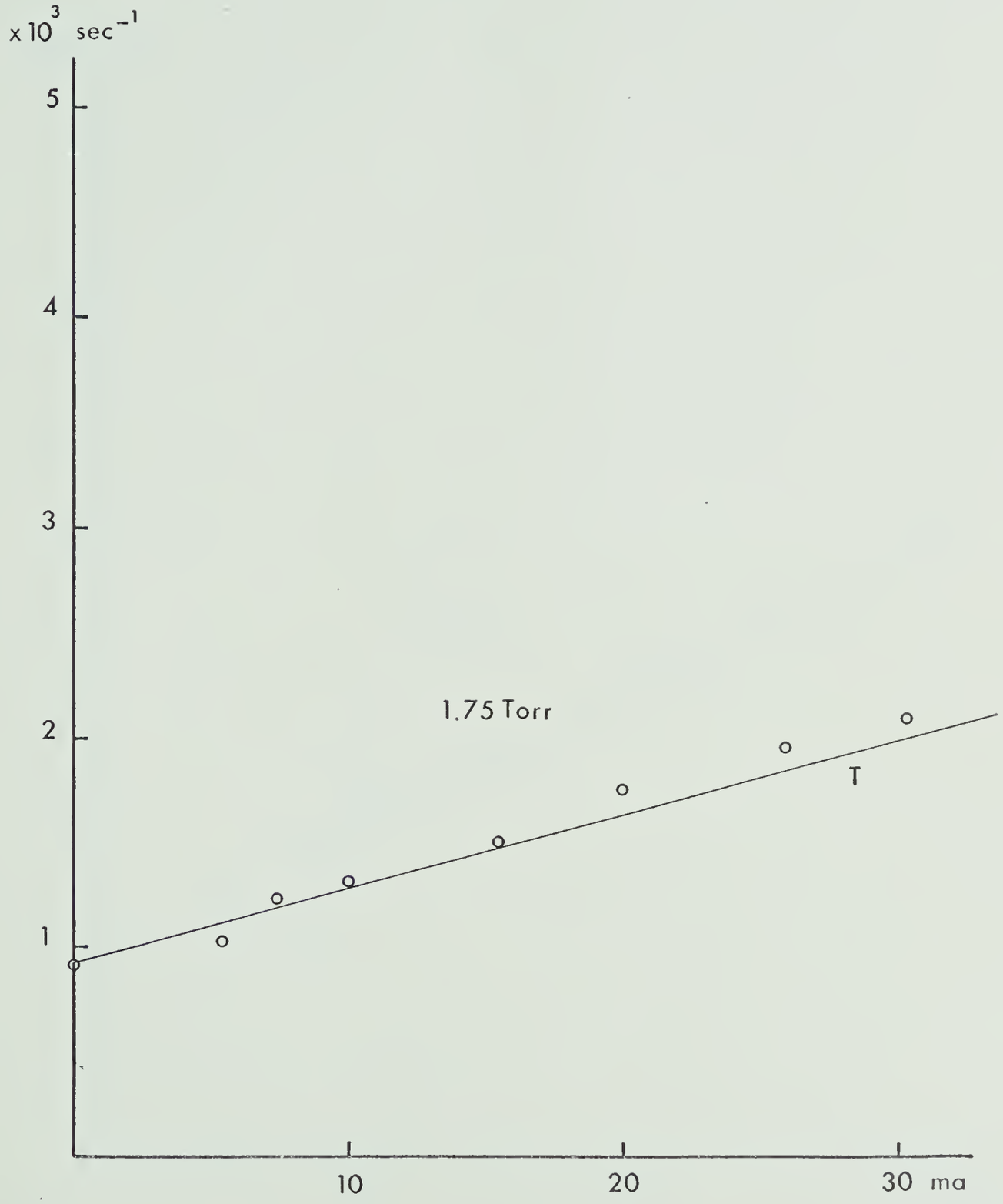

d

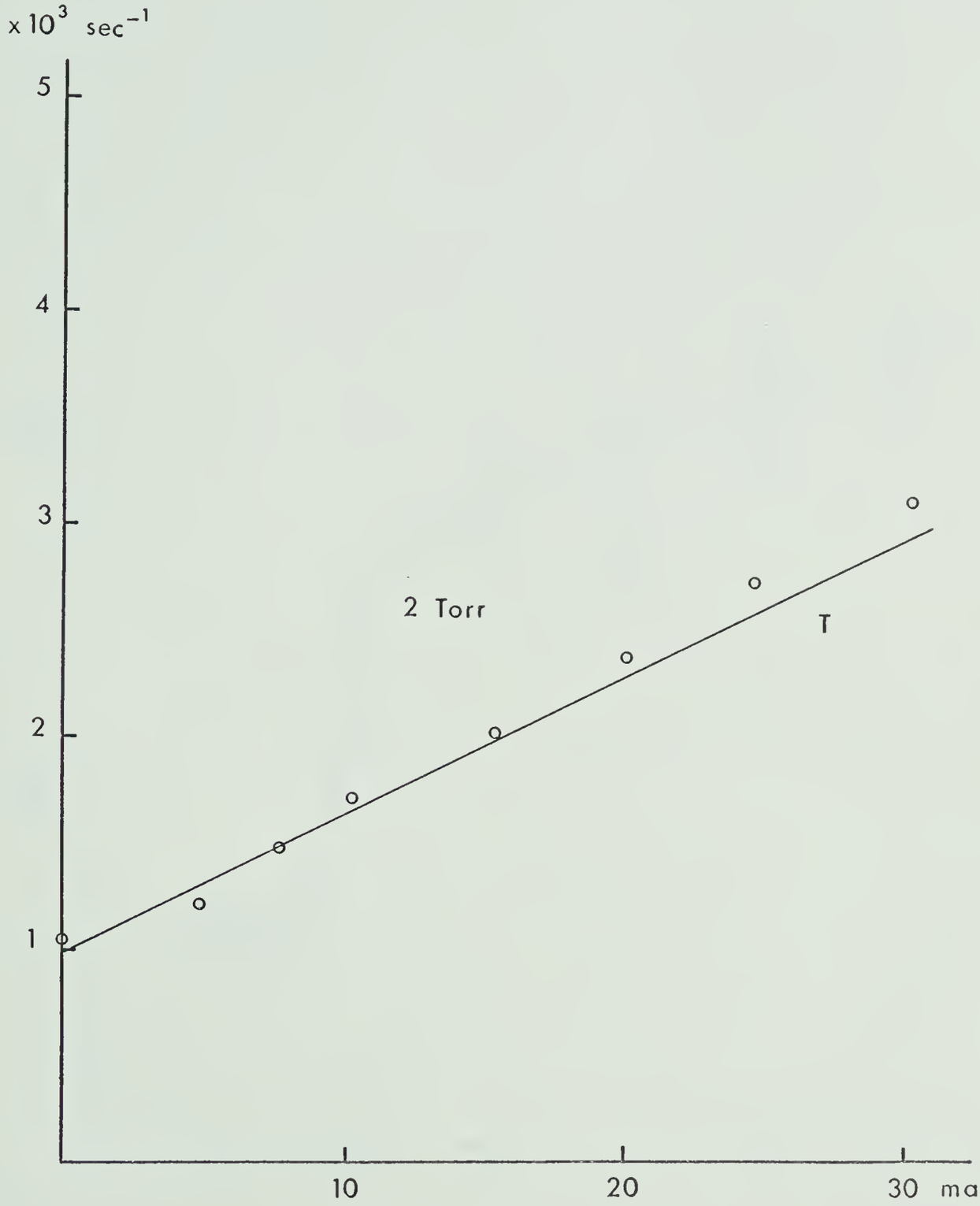

e

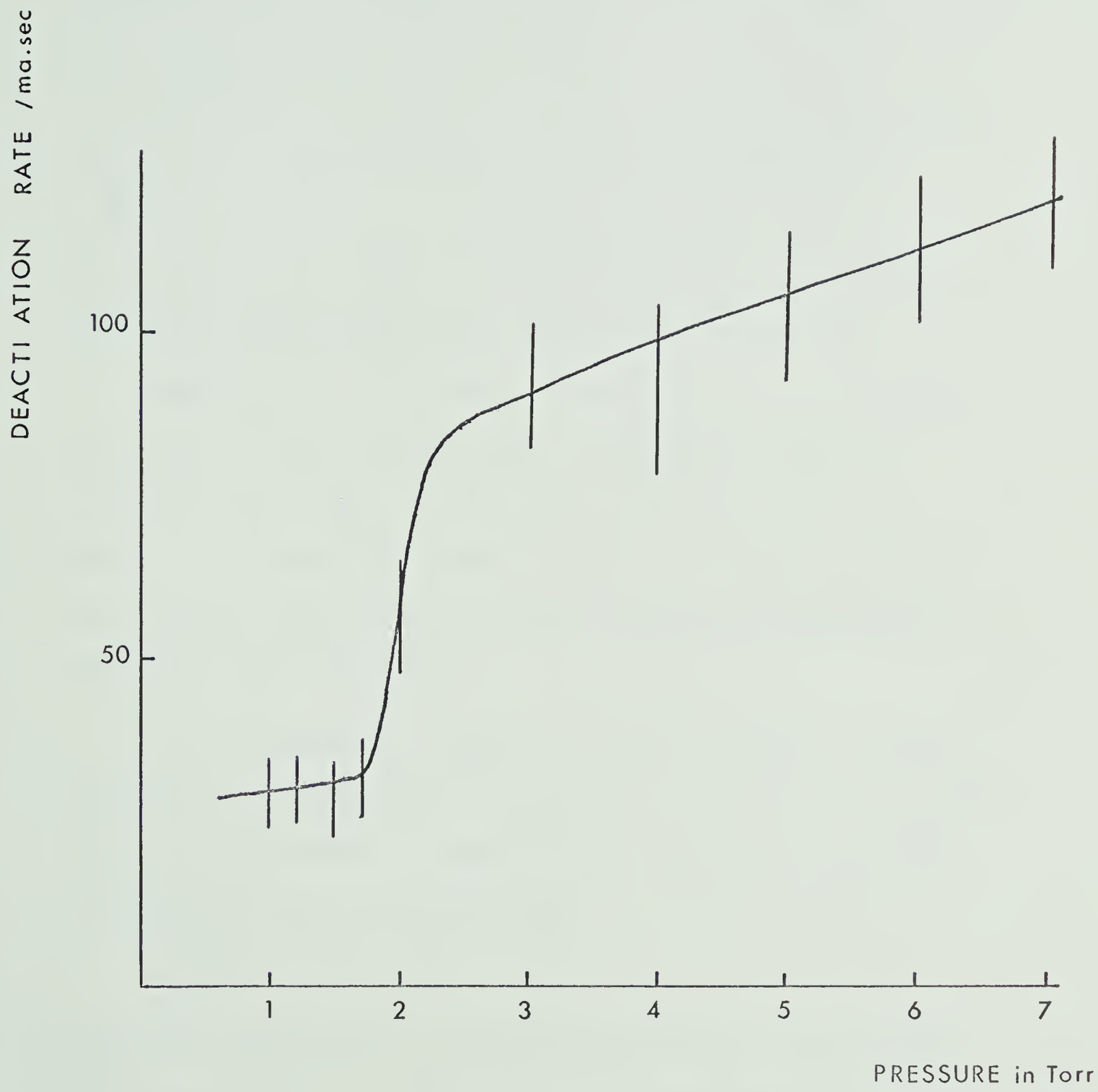

FIG.XVI

In order to obtain this curve, we have subtracted out the temperature dependence of the relaxation rate as given by Rosser et al (Ref. V). It should be pointed out, however, that the measurements of Rosser were obtained in heated gases in thermodynamic equilibrium which is not likely to be the situation prevailing in a glow discharge in our experiment. In this discharge we may assume different vibrational temperatures but not a real equilibrium and as we have seen before $T(001) > T(010) \sim T(100) > T_{tr}$. ; consequently we do not know how this multiple system affects the deactivation rate. The applied temperature compensation is then smaller than the real one.

Comparing Fig. XVI and Fig. X we can see that the transition occurs at 2.25 torr precisely where the fluorescent signal is crossing the zero axis. We know that before this transition $T(001) >> T(100)$ and after $T(001) \sim T(100)$ and it may be possible that such a non-equilibrium vibrational temperature phenomenon influence the deactivation rate..

If, for example, the temperature effect is ignored, electron de-excitation could proceed via collisions of the second kind either direct or by intermediary compound states. Some direct reactions which may occur can be generalized by,

12 $\quad CO_2(001) + e \rightarrow CO_2(NMO) + e + \Delta E$

None of the cross-sections involved above have ever been measured. If we assume the rate of 30/ma. sec to be representative of electron deactivation we can calculate a total cross-section for equation 12. From the measured parameters for our discharge a

cross-section of 10^{-15} cm^2 was calculated which seems quite large compared with usual molecular cross-sections. In fact, a quantum mechanical calculation has been made of the cross-sections for excitation and de-excitation assuming a simple dipole interaction between an electron and a CO_2 molecule. The results are presented in Appendix III.

It therefore seems likely that electron induced vibrational temperature effects are more important than simple de-excitation by collisions of the second kind. Detailed experiments would be necessary to establish the correct explanation for the anomalously large de-excitation rate.

CONCLUSION

Observation of Q-spoiled induced 4.3μ fluorescence, which has been previously applied by Hocker et al, Moore et al and Rosser et al to collisional relation in CO_2, has proved useful in measuring population level and deactivation rates of the (001) state under various laser discharge conditions. Initial measurements made in this experiment gave comparable rates to those previously established for pure CO_2 and CO_2-N_2 mixtures with no discharge present. In addition, a new measurement has yielded a value of 8000 sec^{-1} $torr^{-1}$ for CO_2-CO mixtures.

This technique was also used in a discharge case and has shown that a maximum inversion of population between upper and lower laser levels occurs at 1 torr, followed by a sharp transition at 2.5 torr to the absorption configuration. This transition may possibly be due to a change in the electron energy distribution at this pressure. Interpretation of equipopulation between upper and lower levels has led us to a new measurement of the integrated excitation cross-section of the (001) state which is comparable to that measured by Boness and Schulz. In addition a quantum mechanical calculation was made of the upper level excitation and de-excitation cross-sections; the excitation cross-section shows good agreement with the measured one.

The measured deactivation rate has also shown the same transition behaviour which we attribute to a non thermodynamic equilibrium rather than direct electron de-excitation as a

dominant effect. The important result is that in a typical laser discharge the deactivation rate due to electron processes is of the order of the molecular relaxation one, an effect not established before.

A complete understanding of these phenomena is limited by the lack of knowledge of the electron inelastic processes with CO_2 molecules and the energy distribution of the electrons in such a discharge.

APPENDIX I

Trapping of Radiation (Ref. VI).

We have seen previously that the 4.3μ radiation leading to a transition to ground state is absorbed partially by the gas. This appendix is a study of this effect.

Let us define $T(\rho\nu)$ the probability for a quantum of radiation from a localized source to traverse a distance ρ

1 $$T(\rho\nu) = e^{-k(\nu)\rho}$$

2 $$T(\rho) = \int P(\nu)\, e^{-k(\nu)\rho}\, d\nu$$ where $P(\nu)$ is the emission frequency spectrum.

The absorption constant will be determined by one of :

Natural broadening.

3 $$k(\nu) = \frac{c}{1+\left[\frac{2(\nu-\nu_o)}{\Delta\nu_N}\right]^2} \quad \text{where } \Delta\nu_N = \frac{1}{2\pi\tau}$$

From thermodynamic considerations

4 $$\int k(\nu)\, d\nu = \frac{\lambda_o^2 g_2 N}{8\pi g_1 \tau}$$ τ = lifetime of the transition

gives for the constant C the value

5 $$C = \frac{\lambda_o^2 N g_2}{2\pi g_1}$$ g_1, g_2 statistical weight of the initial and final states

Doppler broadening

6 $$k(\nu) = \frac{\lambda_o^3 N g_2}{8\pi g_1} \frac{1}{\pi^{1/2} v_o \tau} \exp -\left[\left(\frac{\nu-\nu_o}{\nu_o}\right)^2 \frac{c^2}{v_o^2}\right]$$

where $v_o = \left(\frac{2RT}{M}\right)^{\frac{1}{2}}$

This case is going to be discussed in detail later on.

Pressure broadening

7 $$k(\nu) = \frac{c'}{1+\left[\frac{2(\nu-\nu_o)}{\Delta\nu_L}\right]^2}$$ where $\Delta\nu_L = \frac{\nu_c}{\pi}$ and ν_c is the collision frequency

We can now calculate the frequency spectrum of the emitted radiation.

In thermodynamic equilibrium $P(\check{\nu})$ is proportional to $k(\nu)$ and since $\int P(\nu)d\nu=1$

9 $$k(\nu) = \frac{\lambda_o^2}{8\pi}\ \frac{g_2}{g_1}\ \frac{N}{\tau} \qquad P(\nu) = k_1\ P(\nu)$$

Thus

10 $$T(\rho) = \int P(\check{\nu})\ e^{-k_1 P(\nu)}\ d\nu$$

In the case of a Doppler distribution letting $x = \frac{\nu-\nu_o}{\nu_o}\ \frac{c}{\nu_o}$

$$P(x) = \frac{1}{\pi^{\frac{1}{2}}}\ e^{-x^2} \quad \text{and} \quad k(x) = k_o e^{-x^2}$$

Then

11 $$T(\rho) = \frac{1}{\pi^{\frac{1}{2}}} \int_{-\infty}^{+\infty} e^{-x^2}\ \exp\left[-k_o \rho e^{-x^2}\right]\ dx$$

A change of variable $x = \text{Log}\ \frac{\frac{1}{2}k_o\rho}{y}$ gives for $T(\rho)$.

FUNCTION X FOR VARIOUS OPACITY VALUES

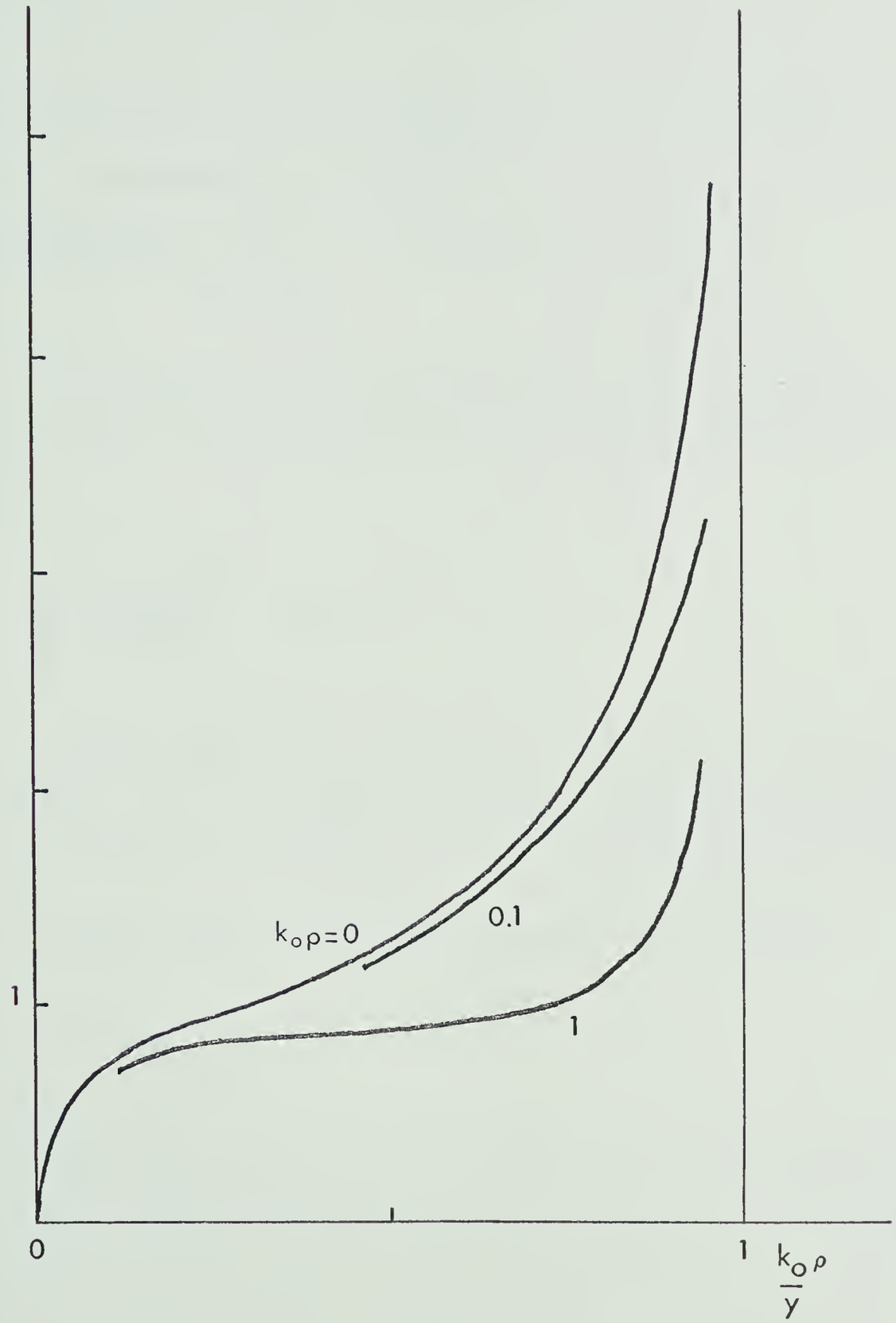

FIG. XVII

$$12 \qquad T(\rho) = \frac{1}{k_o \rho \pi^{\frac{1}{2}}} \int_0^{k_o \rho} \frac{e^{-y}}{(\mathrm{Log} k_o \rho - \mathrm{Log}\ y)^{\frac{1}{2}}}\, dy$$

We are interested in $T(\rho)$ for value of $k_o\rho$ of the order of 1 where no approximation can be used.

The function $X = \dfrac{e^{-y}}{\frac{1}{2} k_o \rho}$ is plotted in Fig. XVII

$\mathrm{Log}\ \dfrac{k_o \rho}{y}$

and $T(\rho)$ was measured from the area under the curve. It can be checked from 12 that the limit of $T(\rho)$ for $k_o\rho \to o$ is equal to one since

$$\int_0^1 \left[\mathrm{Log}\ \frac{1}{x}\right]^{-\frac{1}{2}} dx = \pi^{\frac{1}{2}}$$

$T(\rho)$ is given in Fig. XVIII versus $k_o\rho$. In our case with a pressure range from 1 to 5 torr Doppler broadening predominates and gives a total bandwidth of 116 MHz for the 4.3μ transition at room temperature.

At line center, the Doppler absorption coefficient is

$$13 \qquad k_o = \frac{\lambda_o}{8\pi^{3/2} v_o} \frac{N}{\tau} = 2.3\ 10^{-14} N$$

For (001), J=19 state $N=2.2310^{15}$ at 1 torr, this gives a $k_o\rho$ for 1 cm, of 51 which from Fig. XVIII gives a transmission coefficient of $5\,10^{-3}$. Fig. XIX shows N versus rotational number J for 1 torr, transmission coefficient and signal S which is proportional to T.N.

TRANSMISSION FOR DOPPLER BROADENING

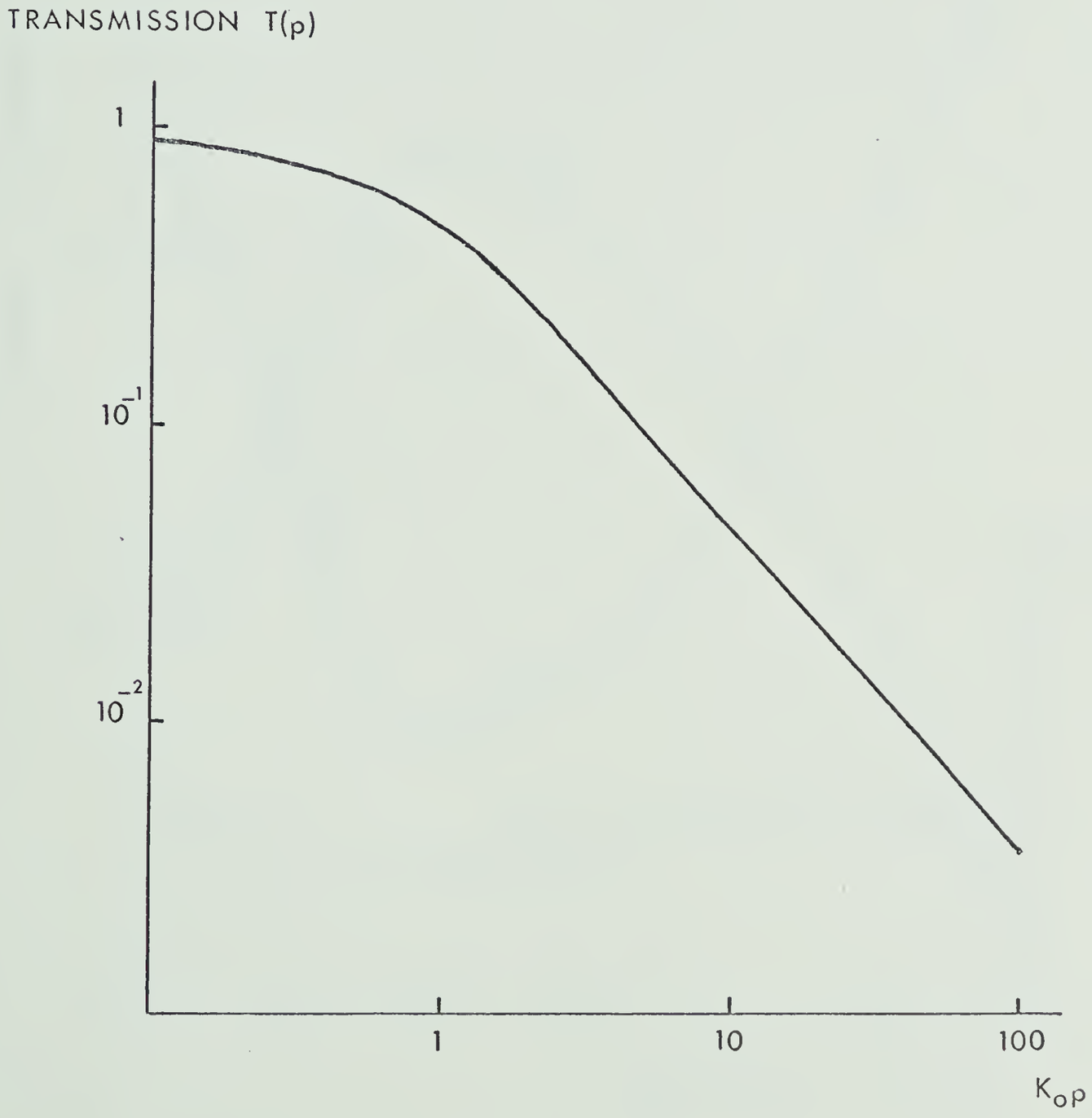

FIG. XVIII

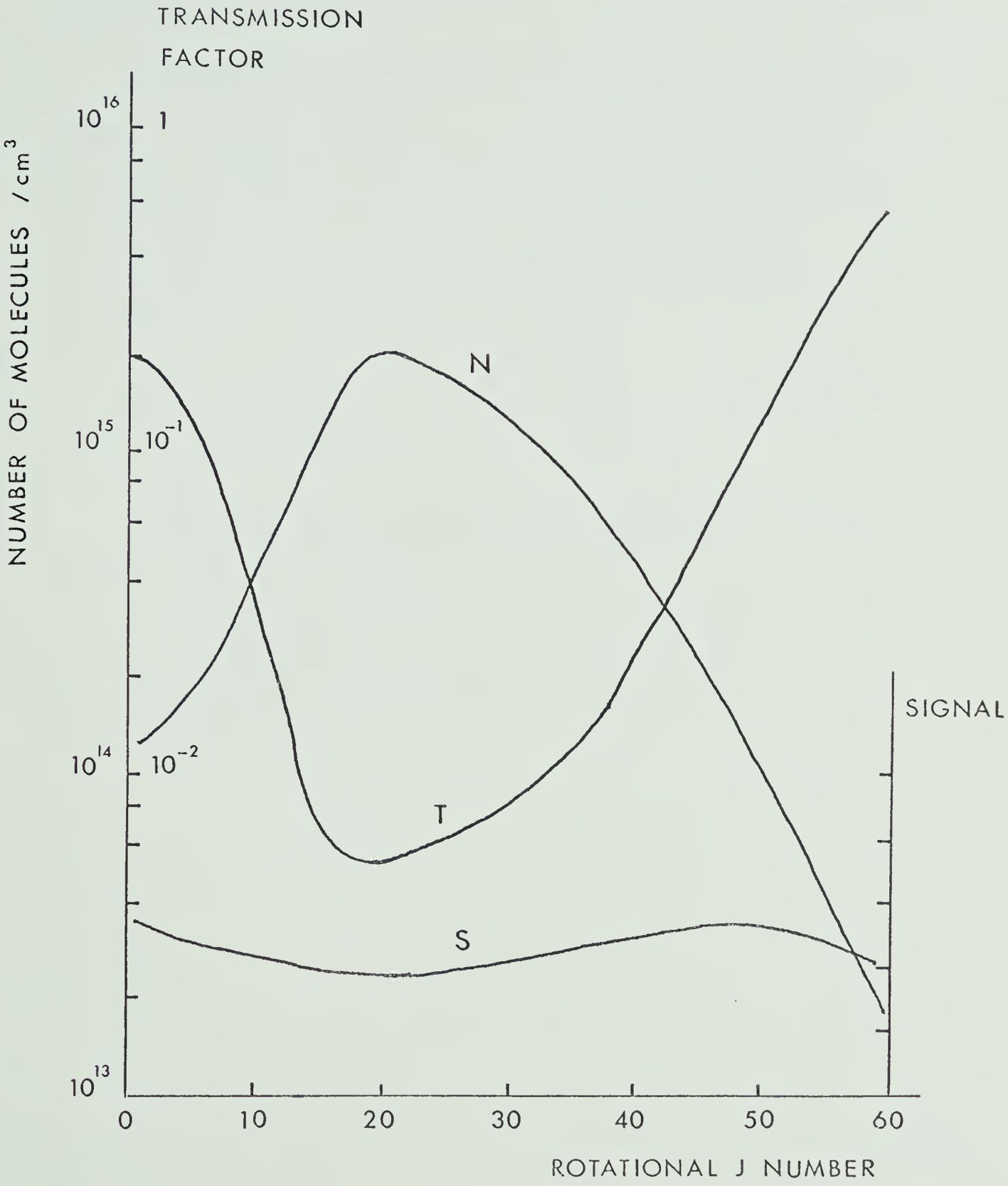
TRANSMISSION
FACTOR
1
10^{-1}
10^{-2}
NUMBER OF MOLECULES / cm^3
10^{16}
10^{15}
10^{14}
10^{13}
N
T
S
SIGNAL
0
10
20
30
40
50
60
ROTATIONAL J NUMBER

FIG.XIX

The maximum of the signal occurs (for 1 cm absorption at 1 torr) at J=0 and J=50 and the integrated signal over all J numbers is 1% of the emitted one.

Trapping has another effect on the signal. The exponential decay is given by $\exp(-\delta g t)$ where $\delta=\frac{1}{\tau}$, τ being the radiative time of an isolated molecule and g "the escape factor" characteristic of the imprisonment process. For a Doppler broadened line and for large $k_o\rho$

$$g = \frac{1.875}{k_o\rho \ (\pi \mathrm{Log}\tfrac{1}{2}k_o\rho)^{\frac{1}{2}}}$$

In our case the predominant signal originates from low J number and J around 50 where $k_o\rho<10$; here we can assume value 1 for g. That means the decay of the signal is very close to the actual radiative decay, which was measured to be 2.5 m sec (see Fig. III).

APPENDIX II

Discussion on the Signal Level.

The level of the signal A is given by,

$$A = NxVx \frac{d\Omega}{4\pi} x \frac{E}{\tau} x\ Sxa$$

where

N = number of molecules radiating from (001) state

V = volume seen by the detector

$d\Omega$ = solid angle of the detector seen by the excited molecules

E = $h\nu$ energy of a 4.3μ photon, $4.2 10^{-20}$ J

τ = the radiative time of the transition, 2.6 m sec

S = sensitivity of the detector (which has been measured using a black body radiator), $2 10^{4}$ volt/watt

a is a factor of transmission.

Half of the signal is lost by reflection or absorption on the salt window of the cell, the 4.3μ filter (see Fig XX) and the calcium fluoride window of the detector. The constant a contains the trapping coefficient depending on the rotational J number (see App I). Thus we find the integrated signal transmitted is 1% of the signal emitted for a 1 torr pressure of CO_2.

If we take the example of 1 torr of CO_2 without any discharge, the signal is 100 μv, from which we can find the number of molecules excited from the (100) to the (001) levels.

For $V = 10cm^3$, $d\Omega = \frac{3}{2500}$, $a = 5\ 10^{-3}$ we find

$$N = 1.810^{-3} N_o \text{ with } N_o = 3.54\ 10^{16}/cm^3$$

At 1 torr and 293°K, however, the number of absorbing molecules in the (100) J=20 state is only 710^{-5}, which is too low for the observed signal by a factor of 25.

This inconsistency can be approximately accounted for if rotational relaxation is included. It has been shown that the rotational relaxation time is of the order of the collision time, which is 10^{-7} sec at 1 torr (see Ref. XIII). Thus for a laser pulse width of 1 μsec, there is sufficient time for cross-relaxation to feed all rotational states to J=20 in absorption.

The results that N is larger than the total number of molecules in the (100) state ($N_{100}=1.15\ 10^{-3}\ N_o$) by a factor of 1.6 may be explained by the imprecision in the determination of the different parameters, or by the influence of the (02°0) level, which is only 106 cm^{-1} away from the (100) and strongly coupled to it by Fermi resonance. The time constant of this phenomenon has never been measured but seems to be of the order of 1 μsec.

Signal dependence on temperature

The dependence on temperature of the population of the (100) level is given by the Maxwell-Boltzmann distribution.

$$N(100) = N_o e^{-\frac{\Delta E}{kT}}$$

RANSMISSION

F THE 4.3μ

ILTER

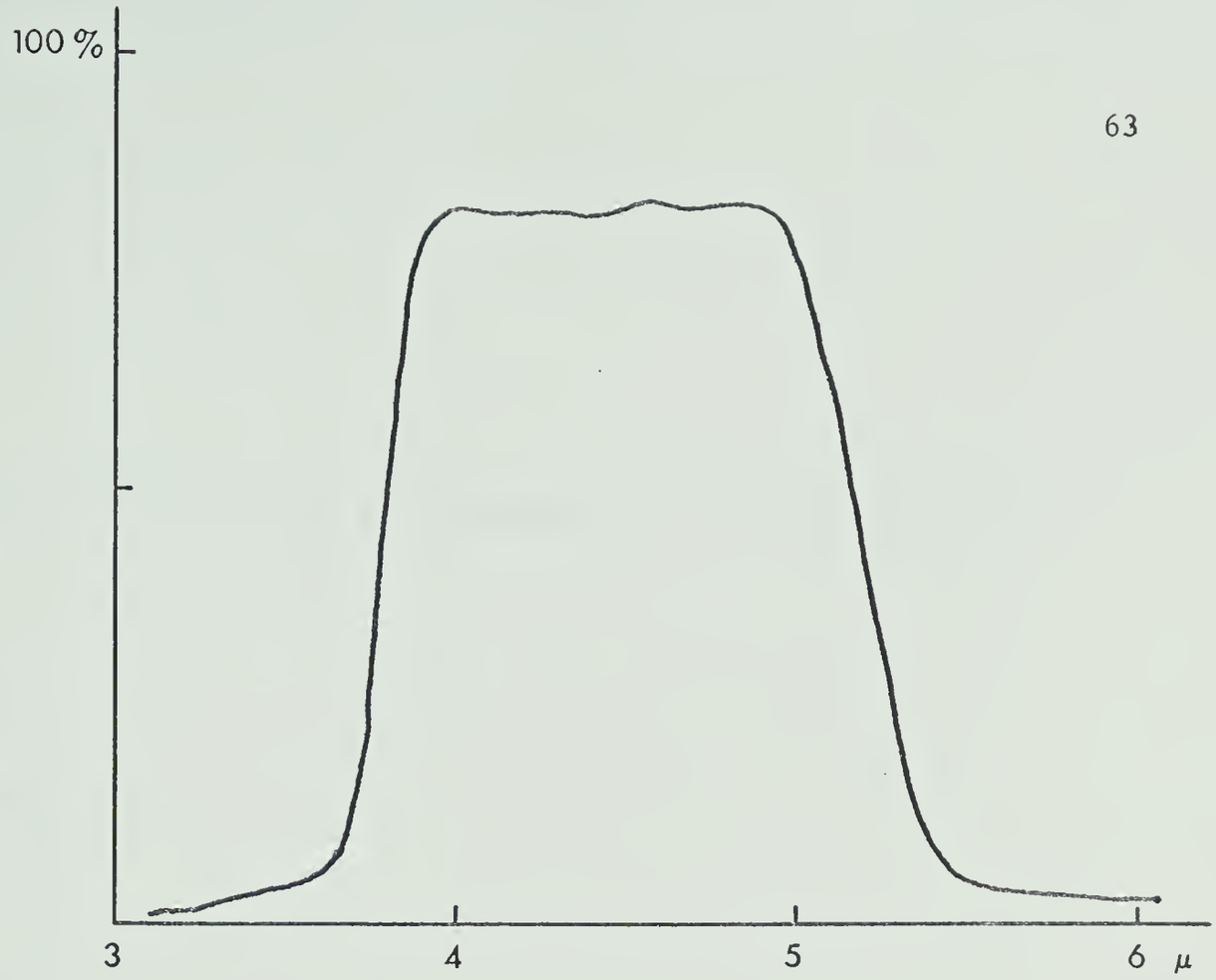

FIG.XX

OSPHERIC CO_2

ORPTION IN THE

NOCHROMATOR

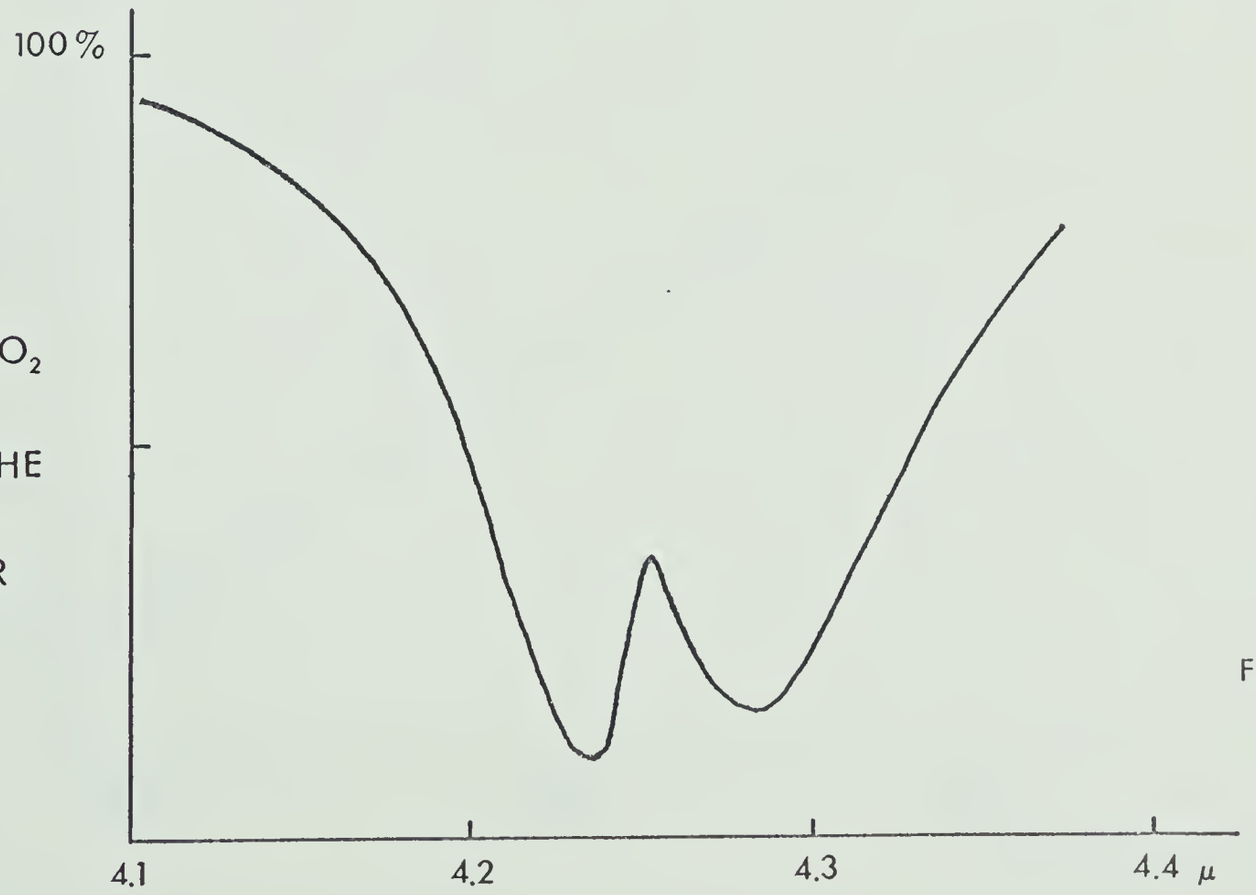

FIG.XXI

CALCULATED SIGNAL DEPENDENCE ON TEMPERATURE

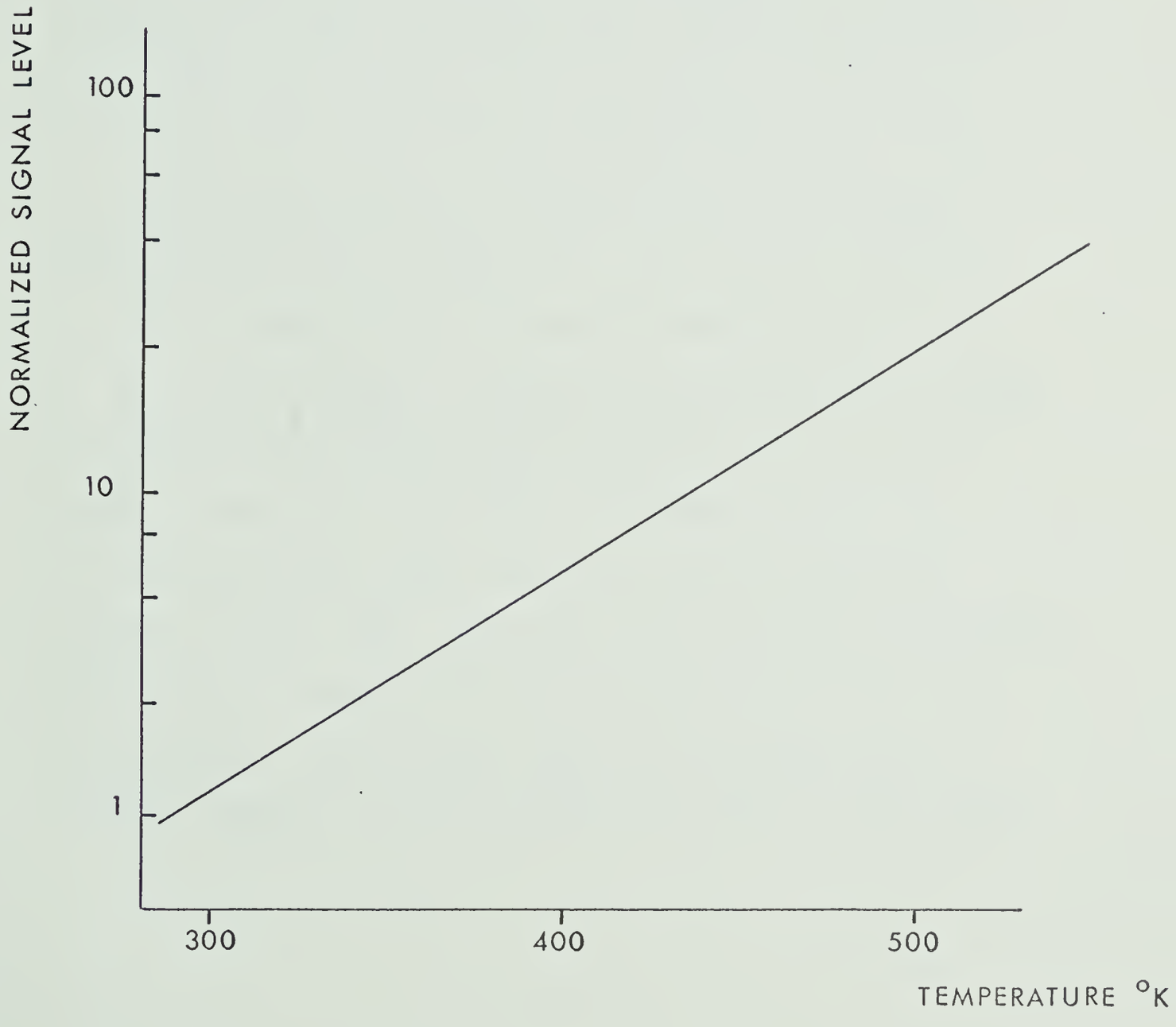

FIG. XXII

The signal being proportional to the (100) population in some cases, it will increase in the same manner (see Fig. XXII).

Use of a monochromator.

If the level of the signal was sufficient we could hope to see the dependence of the signal on the J number and how the energy is spread among the different levels of the asymmetric mode. Although a monochromator could be designed to give this resolution, the signal level would have to be even more enhanced since, when opened at F/7 it does not collect as mush light as the detector. The volume of gas observed is now only 2 cm^3 and $d\Omega$, the solid angle detected is now given by the slit opening which must be 0.4 mm in order to give the necessary resolution of 100Å. In addition, the transmission effeciency is lower than 0.5 for different reasons. Even when the monochromator is flushed with nitrogen the atmospheric CO_2 and its strong bound at 4.3μ absorbs a large part of the signal. This absorption has been measured using a Black Body radiator and a lock-in detection technique (see Fig. XXI). The signal seen through the monochromator would be only a few micro volts, thus buried in the 50 μv noise of our detector. The only hope would be to integrate over a sufficient number of pulses to increase the signal to noise ratio.

Calculation of the Excitation and De-excitation Cross-Sections of the (001) Level.

Results show that even using a rough calculation, dipole point interaction Born approximation and neglecting rotational effects, we can get an idea of the shape of the excitation and de-excitation cross-sections versus the energy of the incident electron. The calculation should be considered a first order approximation to a more correct result which would include rotational and time-dependent potential effects.

Under the assumption of the Born approximation, the interaction potential was taken to be,

$$V(r) = - \frac{M\ e \cos\theta}{r^2}$$

$\vec{q} = \vec{k}_\alpha - \vec{k}_\beta$ is the difference between the two wave vectors defining incident and outgoing plane waves (Ref. XII).

Thus $$\frac{h^2 k_\beta^2}{2m} = \frac{h^2 k_\alpha^2}{2m} \pm E\nu$$

and $$P(k_\alpha, k_\beta, \zeta) = - \frac{m}{2\pi h^2} \int V(r)\ \exp\ (i\ \vec{q}.\ \vec{r})\ dr$$

From which the total inelastic cross-section Σ_T can be computed

$$\sigma_T = \int \frac{k_\beta}{k_\alpha} \left| P \right|^2 \ d\Omega$$

GEOMETRY USED FOR INTEGRATION

OF TRANSITION PROBABILITY

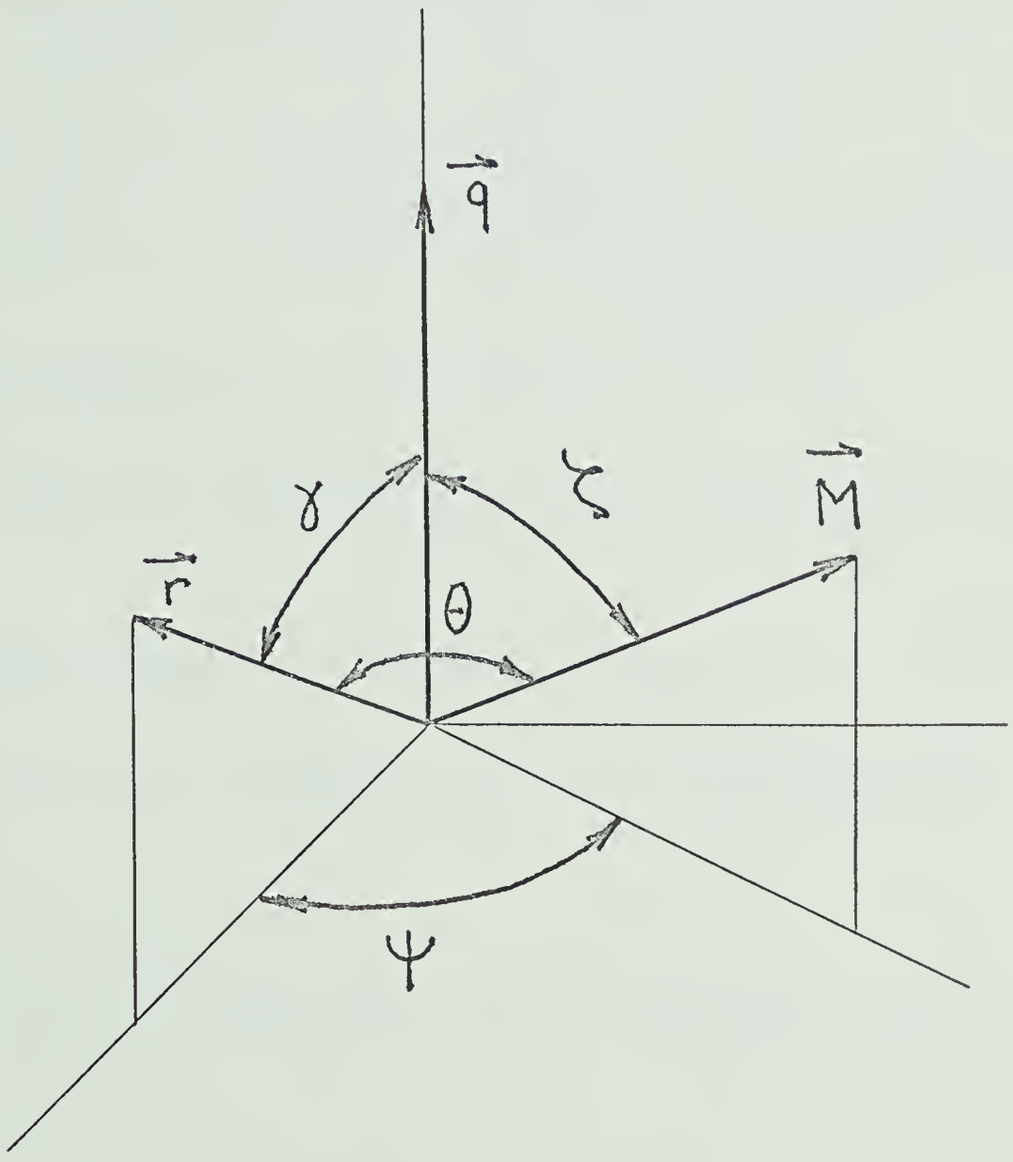

FIG. XXIII

The next part is an integration over all possible spatial configurations. To do this, the angles are defined in Fig. XXIII where $\vec{q}$ is taken as the polar axis and $\vec{r}$ is in the xoz plane The integration is first performed in $\vec{r}$.

Substituting for V(r)

$$P(k_\alpha,k_\beta,\zeta) = \frac{mMe}{2\pi h^2} \int \frac{\cos\theta}{r^2} \exp\,(i\,\vec{q}.\,\vec{r})\,dr$$

Using $\cos\theta = \cos\gamma\cos\zeta + \sin\gamma\sin\zeta\cos\psi$

$$P(k_\alpha,k_\beta,\zeta) = \frac{mMe}{2\pi h^2} \int \frac{\exp\, iqr\,\cos\gamma}{r^2} (\cos\gamma\,\cos\zeta + \sin\gamma\,\sin\zeta\,\cos\psi)\, r^2 dr\, d(\cos\gamma)\, d\psi$$

which integrated over azimuth yields

$$P(k_\alpha,k_\beta,\zeta) = \frac{mMe\,\cos\zeta}{h^2} \int_0^\infty dr \int_0^\pi \exp(iqr\cos\gamma)\,\cos\gamma\, d(\cos\gamma)$$

The last integral can be computed and gives

$$P(k_\alpha,k_\beta,\zeta) = \frac{mMe\,\cos\zeta}{h^2}\, 2i \int_0^\infty \frac{qr\,\cos\,qr - \sin\,qr}{q^2r^2}\, dr$$

change of variable x=qr gives

$$P(k_\alpha,k_\beta,\zeta) = \frac{mMe\,\cos\zeta}{h^2}\, \frac{2i}{q} \int_0^\infty \frac{x\cos x - \sin x}{x^2}\, dx$$

$$P(k_\alpha,k_\beta,\zeta) = \frac{2imMe\,\cos\zeta}{qh^2} \left[\frac{\sin x}{x}\right]_0^\infty$$

which gives

$$P(k_\alpha, k_\beta, \zeta) = - \frac{2i\, mMe\, \cos\zeta}{qh^2}$$

The differential cross-section is then equal to, averaging over all possible dipole orientation.

$$\frac{d\sigma r_T}{d\Omega} = \frac{2\, m^2M^2e^2}{h^4} \int dk \int_o^\pi \frac{k_\beta}{k_\alpha} \frac{\cos^2\zeta}{q^2} \sin\zeta d\zeta$$

which leads to a total cross-section of

$$\sigma_T = \frac{4}{3} \frac{m^2M^2e^2}{h^4} \int \frac{k_\beta}{k_\alpha} \frac{1}{q^2} d\Omega \quad \text{with } d\Omega = 2\pi \sin\phi d\phi$$
$$\vec{q} = \vec{k}_\beta - \vec{k}_\alpha$$

Finally substituting

$$q^2 = k_\beta^2 + k_\alpha^2 - 2k_\beta k_\alpha \cos\phi \text{ and } 2qdq = 2k_\beta k_\alpha \sin\phi d\phi$$

$$\int \frac{k_\beta}{k_\alpha} \frac{d\Omega}{q^2} = \frac{2\pi}{k_\alpha^2} \int_{k_\beta - k_\alpha}^{k_\beta + k_\alpha} \frac{dq}{q}$$

we obtain

$$\sigma_T = \frac{8\pi}{3} \frac{m^2M^2e^2}{h^4} \frac{1}{k_\alpha^2} \text{Log} \frac{k_\beta + k_\alpha}{k_\beta - k_\alpha} \quad \text{with } k_\beta^2 - k_\alpha^2 = \pm \frac{2mE\nu}{h^2}$$

By putting numerical values and replacing k_α by E the incident energy in ev we get

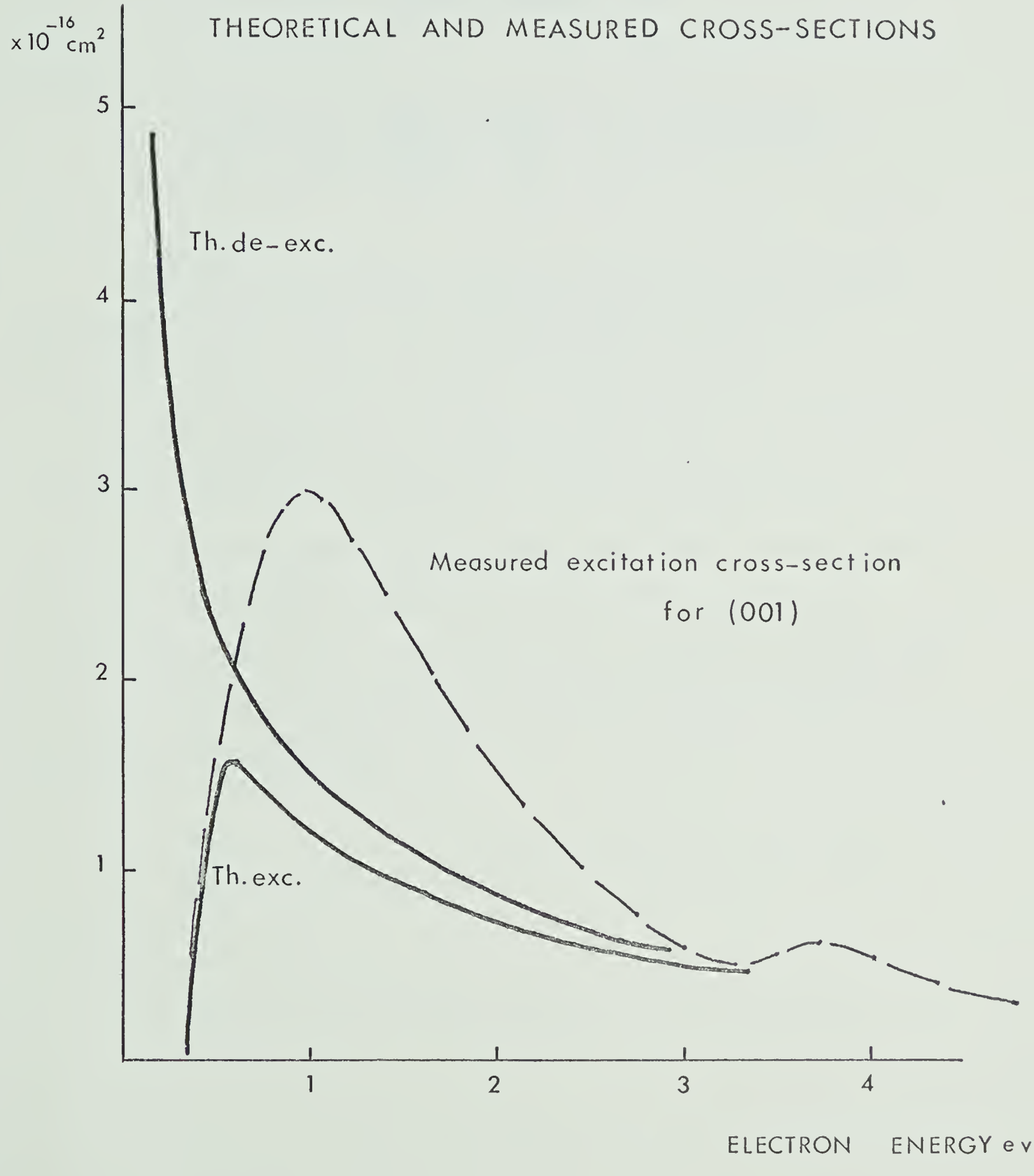
THEORETICAL AND MEASURED CROSS-SECTIONS
x 10⁻¹⁶ cm²
5
4
3
2
1
Th. de-exc.
Measured excitation cross-section
for (001)
Th. exc.
1
2
3
4
ELECTRON ENERGY ev

FIG. XXIV

$$\sigma_T = 5\ 10^{-17}\ \frac{1}{E}\ \text{Log}\ \frac{\sqrt{E}\ +\sqrt{E-E\nu}}{\sqrt{E}\ -\sqrt{E-E\nu}}$$ for the excitation cross-section

and

$$\sigma_T = 5\ 10^{-17}\ \frac{1}{E}\ \text{Log}\ \frac{\sqrt{E+E\nu}\ +\sqrt{E}}{\sqrt{E+E\nu}\ -\sqrt{E}}$$ for de-excitation

These two curves and the measured one by Boness and Schulz are shown in Fig. XXIV. Our calculation under estimates the excitation cross-section but agrees to within a factor of 2 which is very good considering the assumptions made above. For a lev Maxwellian distribution of electrons, the de-excitation cross-section should be approximately 5 times larger than the excitation one, still too small to explain the rate of 30/ma.sec measured before (see chapter III). But here we have considered de-excitation to the ground state which is only one possible path for deactivation by electrons (see eq. 12).

I G. Herzberg:

Infra-red and Raman Spectra of Polyatomic Molecules (D. Van Nostrand Co., Inc., New York).

II L.O. Hocker, M.A. Kovacs, C.K. Rhodes, G.W. Flynn and A. Javan :

Vibrational Relaxation Measurements in CO_2 Using an Induced-Fluorescence Technique. Phys. Rev., Vol.17 Number 5 pp 233 (1966).

III G.W. Flynn, L.O. Hocker, A. Javan, M.A. Kovacs and C.K. Rhodes :

Progress and Applications of Q-Switching Techniques Using Molecular Gas Lasers. IEEE J of QE 1966 pp 378.

IV C.B. Moore, R.E. Wood, B.L. Hu and J.T. Yardley :

Vibrational Energy Transfer in CO_2 Lasers, J of Chem. Phys. Vol. 46 Number 11 pp 4222 (1967).

V W.A. Rosser, A.D. Wood and E.T. Gerry :

Deactivation of Vibrationally Excited CO_2. J of Chem. Phys. Vol. 50 Number 11 pp 4996 (1969).

VI T. Holstein :

Imprisonment of Resonant Radiation in Gases. Phys. Rev. Vol. 72 Number 12, pp 1212 (1947) and Phys. Rev. Vol. 83 Number 6, pp 1159 (1951).

VII R.D. Hake and A.V. Phelps :

Momentum Transfer and Inelastic Collision Cross-Sections For Electrons in O_2, CO and CO_2, Phys. Rev. Vol. 158 Number 1 pp 70 (1967).

VIII M.J.W. Boness and G.J. Schulz :

Vibrational Excitation of CO_2 by Electron Impact, Phys. Rev. Letters, Vol 21 pp 1031 (1968).

IX W.E.K. Gibbs and H.A. Kellock :

Current Dependant Decay of CO_2 (001) Level in Pulsed CO_2-N_2 Mixtures. Phys. Letters. Vol. 29a. Number 4 pp 190 (1969).

X A. Andrick, D. Danner and H. Ehrhardt :

Vibrational Excitation of CO_2 by Dipole Interaction With Slow Electrons. Phys. letters Vol 29a, Number 6, pp 346 (1969).

XI R.L. Taylor and S. Bitterman :

Survey of Vibrational Relaxation Data for Processes Important in the CO_2-N_2 Laser System. Rev. of Mod. Phys. Vol. 41, Number 1 pp 26 (1969).

XII Sharma and C.A. Brau :

Energy Transfer in Near Resonant Molecular Collisions Due to Long-Range Forces with Application to Transfer of Vibrational Energy from ν_3 Mode of CO_2 to N_2. J of Chem. Phys. Vol. 50, Number 2 pp 924 (1969)

XIII P.K. Cheo and R.L. Abrams :

Rotational Relaxation Rate of CO_2 Laser Levels.Applied Physics Letters. Vol. 14, pp. 14 (1969).

XIV W.A. Rosser and E.T. Gerry :

De-excitation of VIbrationally Excited CO_2. J of Chem. Phys. Vol. 51, pp. 2286. (1969).

XV L.B. Loeb :

Basic Processes of Gaseous Electronics. University of California Press (1961).

XVI G.J. Schulz and S.C. Brown :

Microwave Study of Positive Ion Collection by Probes. Phys. Rev. Vol. 98 Number 6. pp 1642 (1955).